

A Latent Causal Inference Framework for Ordinal Variables

Martina Scauda

MS2985@CAM.AC.UK

Dep. of Mathematics and Computer Science, University of Basel, Basel, Switzerland

Dep. of Pure Mathematics and Mathematical Statistics, University of Cambridge, Cambridge, UK

Jack Kuipers

JACK.KUIPERS@BSSE.ETHZ.CH

Dep. of Biosystems Science and Engineering, ETH Zurich, Basel, Switzerland

Giusi Moffa

GIUSI.MOFFA@UNIBAS.CH

Dep. of Mathematics and Computer Science, University of Basel, Basel, Switzerland

Abstract

Ordinal variables, such as on the Likert scale, are common in applied research. Yet, existing methods for causal inference tend to target nominal or continuous data. When applied to ordinal data, this fails to account for the inherent ordering or imposes well-defined relative magnitudes. Hence, there is a need for specialised methods to compute interventional effects between ordinal variables while accounting for their ordinality. One potential framework is to presume a latent Gaussian Directed Acyclic Graph (DAG) model: that the ordinal variables originate from marginally discretizing a set of Gaussian variables whose latent covariance matrix is constrained to satisfy the conditional independencies inherent in a DAG. Conditioned on a given latent covariance matrix and discretisation thresholds, we derive a closed-form function for ordinal causal effects in terms of interventional distributions in the latent space. Our causal estimation combines naturally with algorithms to learn the latent DAG and its parameters, like the Ordinal Structural EM algorithm. Simulations demonstrate the applicability of the proposed approach in estimating ordinal causal effects both for known and unknown structures of the latent graph. As an illustration of a real-world use case, the method is applied to survey data of 408 patients from a study on the functional relationships between symptoms of obsessive-compulsive disorder and depression.

Keywords: Causal inference, Causal diagrams, Latent graphical models, Directed acyclic graph-probit, Ordinal data.

1 Introduction

Ordinal or ordered categorical variables, which take categorical values following an intrinsic listing order, are common in many research fields (Agresti, 2010). Examples include letter grades (A, B, C, D, E, F), survey questions on a Likert scale (strongly disagree, disagree, undecided, agree, strongly agree), stages of cancer (I, II, III, IV); as well as discretized continuous data, such as age groups (children, youth, adults, seniors). The latent continuous underlying construct may be unavailable or non-observable for practical or confidentiality reasons. In such a context, for analysing their ordinal values it is natural to conceptualise them as obtained by marginally discretizing a set of latent continuous variables.

Given the ubiquity of ordinal data, developing interpretable and robust methodologies for defining and inferring causal effects of interventions on ordinal outcomes is of high relevance. Because of inherent technical difficulties, much of the causal inference literature treats ordinal data as nominal or continuous, either ignoring the inherent order among the

categories or assuming that the scale between ordinal levels corresponds to well-defined relative magnitudes.

Under the potential outcomes framework (Splawa-Neyman et al., 1923; Rubin, 1974), causal effects are usually defined as comparisons between the potential outcomes under the two levels of a binary treatment. For an ordinal response, the most common parameter of interest, the average causal effect, is not well-defined since a notion of average only exists for continuous and binary outcomes, where the average is the proportion. Analogously, other measures of centrality do not work with an ordinal response because the scale of the categories is not well defined. For these reasons, most of the literature has focused on binary outcomes (Rosenbaum and Rubin, 1983) as a special case of ordinal ones, with some exceptions. Notable examples include Rosenbaum (2001), who explored causal inference for ordinal outcomes under the assumption of monotonicity, stating that the treatment has a non-negative effects for all units; Agresti (2010) and Agresti and Kateri (2017) who examined a range of ordinal effect measures while assuming independence between potential outcomes; and Volfovsky et al. (2015) who adopted a Bayesian approach that required specifying a full parametric model for the joint distribution of potential outcomes. In the setting of randomized trials, Díaz et al. (2016) proposed a robust causal parameter that avoided reliance on the proportional odds model assumption. Another challenge arises with ordinal treatments since, in the context of the potential outcomes framework, the estimation is often performed using propensity score methods, which are generally confined to binary treatment scenarios. For univariate ordinal treatment variable, Joffe and Rosenbaum (1999) proposed an extension of the propensity score method and Imai and Van Dyk (2004) generalized it to arbitrary treatment regimes (including ordinal and even multivariate) by using propensity functions. As an alternative, Imbens (2000) adopted inverse probability weighting for estimating causal effects from ordinal treatments.

Alongside the potential outcomes framework, causal diagrams, represented by directed acyclic graphs (DAGs) provide a complementary approach to causal inference. Using causal diagrams to describe a data-generating mechanism is appealing as the edges may naturally encode causal links between the variables represented by the nodes on the graph. For a known causal DAG, the intervention calculus (Pearl, 2009) provides a machinery to determine the causal effects of one variable on another. In more common practical situations a suitable causal diagram is rarely known, so we need methods that can learn both a network structure and its parameters from data, keeping in mind that observational data only identify the DAG describing their joint distribution up to its Markov equivalence class (Verma and Pearl, 1990), which we may represent as a completed partially directed acyclic graph (CPDAG).

Learning Bayesian networks intrinsically depends on the data type with existing solutions mainly focused on continuous and nominal data (Rios et al., 2021; Kitson et al., 2023). In the case of Gaussian data, to overcome the lack of knowledge about the graphical structure Maathuis et al. (2009) provide lower bounds for the causal effects after finding a Markov equivalence class compatible with the data. By adopting a Bayesian approach, one can integrate structure learning and effect estimation into a procedure that yields the posterior distribution of causal effects. A key advantage is that the method captures both the graphical and parameter uncertainty, as originally proposed and illustrated in a psychology application by Moffa et al. (2017) for binary data. Later works extended this Bayesian

procedure to dynamic Bayesian networks (Kuipers et al., 2019) and linear Gaussian models (Viinikka et al., 2020).

Until recently, the literature on causal graphical models has given little consideration to the problem of determining a suitable causal graphical framework for ordinal data while coherently defining and evaluating ordinal causal effects. For the structure learning part, Luo et al. (2021) designed an Ordinal Structural EM (OSEM) algorithm accounting for the ordinality through a *latent Gaussian DAG-model*. The parametrization relies on a multivariate probit model, where each ordinal variable is the marginal discretization of a latent Gaussian variable, with their joint Gaussian distribution factorising according to a DAG. In a similar vein, Castelletti and Consonni (2021) assumed a DAG-probit model to evaluate intervention effects in a Bayesian framework, in the special case when the intervention variables are continuous and the response is binary. They model the binary outcome as a discretised instance of a continuous underlying variable, whose distribution, jointly with the remaining continuous variables, is Gaussian and obeys the conditional independence relationships inherent in a DAG. Since binary variables are a special case of ordinal variables, the more general latent Gaussian DAG-model adopted in Luo et al. (2021) encompasses the *Probit DAG-model* considered in Castelletti and Consonni (2021).

Recently Grzegorzczak (2024) proposed a Bayesian version of the OSEM algorithm (Luo et al., 2021), while Castelletti (2023) extended the structural recovery approach of Castelletti and Consonni (2021) to deal with mixed data, including ordinal. Nevertheless, the causal graphical framework still lacks a methodology to determine the causal effect on an ordinal outcome following an intervention on another binary or potentially ordinal variable.

Realizing the theoretical gap in this matter and building on the multivariate probit regression models of Albert and Chib (1993) and the latent Gaussian modelling of Luo et al. (2021), we develop an order-preserving methodology to compute interventional effects among ordinal variables in a latent Gaussian DAG model. The rest of the article is organized as follows. In Section 2, we provide an overview of previous approaches including both potential outcomes and causal diagrams, along with latent Gaussian DAG modelling. In Section 3, we present our original contribution with the definition of ordinal causal effect, and how to evaluate it in the proposed latent Gaussian DAG framework. In Section 4, we use synthetic and real data from McNally et al. (2017) to illustrate the performance of our proposed methodology in terms of causal effect estimation with known and unknown latent DAG structures. Lastly, in Section 5, we discuss our results in relation to previous approaches and highlight possible extensions of the present work.

2 Background

Let $\mathbf{X} = (X_1, \dots, X_n)^\top$ be a collection of n ordinal variables, where X_m takes values in the set $\{\tau(m, 1), \dots, \tau(m, L_m)\}$ with $\tau(m, 1) < \dots < \tau(m, L_m)$, $m = 1, \dots, n$. Each variable is assumed to be at least binary, meaning the number of levels $L_m \geq 2$. It is conventional to set $\tau(m, j) = j - 1$ for all $1 \leq j \leq L_m$.

We are interested in the causal effect on an outcome variable X_o of a deterministic intervention on an intervention variable X_i . To describe intervention effects we use Pearl’s do-operator (Pearl, 2009) where the distribution of X_o under an intervention on X_i is generally denoted as $\mathbb{P}(X_o = x_o \mid \text{do}(X_i = x_i))$. Distributional changes or distribution shifts

in the outcome variable between different levels of the intervention variable often constitute target estimands of practical relevance (Holland, 1988). Evaluating and comparing the change in the probability of X_o belonging to level k , when setting the intervention variable X_i to level l' vs level l provides a measure of the distribution shift

$$\mathbb{P}\left[X_o = \tau(o, k) \mid \text{do}(X_i = \tau(i, l'))\right] - \mathbb{P}\left[X_o = \tau(o, k) \mid \text{do}(X_i = \tau(i, l))\right] \quad (1)$$

for each $l \neq l'$ and $l, l' \in \{1, \dots, L_i\}$ and $k \in \{1, \dots, L_o\}$. Our objective is to evaluate *ordinal causal effects* (OCEs) as represented by the target causal estimands in Eq. (1).

2.1 Related Work

Consider a study with N units, an ordinal outcome X with K observed levels and a binary treatment. Under the stable unit treatment value assumption (SUTVA) (Imbens and Rubin, 2015), we can define the pair of potential outcomes $\{X_m(1), X_m(0)\}$ of unit m under treatment and control. In this framework, we can consider causal estimands for ordinal outcomes on either the observed scale or the latent scale. In the latter, there is a pair of latent potential outcomes $(Z_m(1), Z_m(0))$ for each unit m and a deterministic function $g(\cdot)$ which maps them into the observed scale as $X_m(1) = g(Z_m(1))$ and $X_m(0) = g(Z_m(0))$. If the map g is known explicitly or fully identified, the continuous latent potential outcomes can be treated as the actual outcomes and causal analysis reduces to the classical results for continuous potential outcomes (Imbens and Rubin, 2015). In practice, g is often inferred from data and likely its location and scale lack identifiability, key features needed to define meaningful estimands on the latent scale. Nonetheless, Volfovsky et al. (2015) adopts a latent variable formulation to determine posterior predictive estimates of the induced estimands on the observed scales.

On the observed scale instead, the joint distribution of the potential outcomes, which contains complete information about any causal effect, can be summarized by a matrix \mathbf{P} with entries $p_{kl} = \mathbb{P}(X(0) = k, X(1) = l)$ $k, l = 0, \dots, K - 1$, that are the proportions of units whose potential outcomes take on those categories. All estimands are therefore functions of the matrix \mathbf{P} . Since the relative magnitudes between the pair of categories are not defined for ordinal data, a meaningful one-dimensional summary should summarise the differences between the marginal distributions of the potential outcomes. However, this is often insufficient to characterize causal effects and multidimensional estimands are required, such as distributional causal effects (Ju and Geng, 2010)

$$\Delta_j = \mathbb{P}[X_m(1) \geq j] - \mathbb{P}[X_m(0) \geq j] = \sum_{k \geq j} \sum_{l=0}^{K-1} p_{kl} - \sum_{l \geq j} \sum_{k=0}^{K-1} p_{kl}, \quad (2)$$

which measure the difference between the marginal distributions of the potential outcomes at different levels j , similarly to the effects discussed in Boes (2013). Nonetheless, unless those effects have the same sign for all j , it is difficult to select the preferable treatment.

Another possible solution to measure the magnitude of the effect relative to treatment is to use causal estimands that conditions on the level of the potential outcome under control, such as K -dimensional summaries of the form $M_{1i} = \text{median}[X(1) \mid X(0) = j]$ or $M_{2i} = \text{mode}[X(1) \mid X(0) = j]$ ($j = 0, \dots, K - 1$) (Volfovsky et al., 2015). As underlined

by Lu et al. (2018), both the previous estimands are not direct measures of the treatment effect. Moreover, the conditional medians may not be unique and they are only well-defined for the levels j such that the sum of the j -th column of \mathbf{P} is positive.

Alternatively, Lu et al. (2018) propose the following two causal estimands for ordinal outcomes, which measure the probabilities that the treatment is beneficial and strictly beneficial for the experimental units respectively.

$$\iota = \mathbb{P}[X_m(1) \geq X_m(0)] = \sum_{k \geq l} \sum p_{kl}, \quad \eta = \mathbb{P}[X_m(1) > X_m(0)] = \sum_{k > l} \sum p_{kl} \quad (3)$$

Alternatively, Agresti and Kateri (2017) used the relative treatment effect for ordinal outcomes defined as

$$\gamma = \mathbb{P}[X_m(1) > X_m(0)] - \mathbb{P}[X_m(1) < X_m(0)] = \iota + \eta - 1 \quad (4)$$

When $K = 2$ (i.e. X is binary), the relative treatment effect reduces to

$$\gamma = \mathbb{E}[X_m(1) - X_m(0)] = \mathbb{E}[X_m(1)] - \mathbb{E}[X_m(0)] \quad (5)$$

which is exactly the average treatment effect. Since these estimands depend on the association between the two potential outcomes, they are not identifiable from observed data. Under the partial identification strategy of Manski (2003), Lu et al. (2018) derive sharp bounds on ι and η in closed form. Lu et al. (2020) extend these bounds to γ , while Chiba (2018) propose a Bayesian approach requiring a prior on the joint distribution of potential outcomes.

Estimating causal effects for ordinal variables in a latent Gaussian DAG model is closely related to estimating effects under the assumption of Gaussianity. Therefore we start by defining graphical models and causal effects in a Gaussian set-up and build on it for defining and evaluating effects with ordinal data. To fix the notation we start by defining graphical models and briefly introducing general intervention calculus, closely following Pearl (2009).

2.2 Graphical Models and Causal Effects

Let $\mathcal{G} = (V, E)$ be a DAG, with $V = \{1, \dots, n\}$ denoting the finite set of vertices (or nodes) and $E \subset V \times V$ the set of directed edges, whose elements are $(h, j) \equiv h \rightarrow j$ such that $(h, j) \in E$ but $(j, h) \notin E$. Moreover, \mathcal{G} contains no cycles, i.e. paths of the form k_0, k_1, \dots, k_m such that $k_0 \equiv k_m$. For a given vertex j , node h is called a parent of j and node j a child of h if $(h, j) \in E$. The parent set of a node j is denoted by $\text{pa}(j)$.

We consider a collection of n random variables $\mathbf{Y} = (Y_1, \dots, Y_n)^\top$ and assume that their joint p.d.f. $f(\mathbf{y})$, fully characterised by a set of parameters θ , is Markovian with respect to the DAG \mathcal{G} , meaning it factorises as

$$f(y_1, \dots, y_n \mid \theta, \mathcal{G}) = \prod_{m=1}^n f(y_m \mid y_{\text{pa}(m)}, \theta_m, \mathcal{G}) \quad (6)$$

where \mathbf{y} is a realization of \mathbf{Y} , $\theta = \cup_{m=1}^n \theta_m$ and the subsets $\{\theta_m\}_{m=1}^n$ are assumed to be disjoint. The pair $\mathcal{B} = (\mathcal{G}, \theta)$ denotes a Bayesian network, a specific family of probabilistic

graphical model where the underlying structure is a DAG (see Section 3.2.2 of Lauritzen, 1996). From this point forward, all arguments implicitly condition on a given DAG \mathcal{G} , without explicitly indicating it in the notation.

The joint distribution $f(\mathbf{y})$ constitutes the observational (or pre-intervention) distribution. To denote a deterministic intervention on a variable $Y_i, i \in \{1, \dots, n\}$, Pearl (2009) introduced the do-operator $\text{do}(Y_i = y'_i)$, which consists in enforcing $Y_i = y'_i$ uniformly over the population. For a Markovian model, the post-intervention density is then given by the following truncated factorization formula:

$$f(y_1, y_2, \dots, y_n \mid \text{do}(Y_i = y'_i)) = \begin{cases} \prod_{j \neq i} f(y_j \mid y_{\text{pa}(j)}) & \text{if } y_i = y'_i \\ 0 & \text{if } y_i \neq y'_i \end{cases} \quad (7)$$

where $f(y_j \mid y_{\text{pa}(j)})$ are the pre-intervention conditional distributions.

The post-intervention distribution of a variable Y_j with $j \neq i$ is then obtained by integrating out $y_1, \dots, y_{j-1}, y_{j+1}, \dots, y_n$ in Eq. (7), simplifying to

$$f(y_j \mid \text{do}(Y_i = y'_i)) = \begin{cases} f(y_j) & \text{if } Y_j \in y_{\text{pa}(i)} \\ \int f(y_j \mid y'_i, y_{\text{pa}(i)}) f(y_{\text{pa}(i)}) dy_{\text{pa}(i)} & \text{if } Y_j \notin y_{\text{pa}(i)} \end{cases} \quad (8)$$

where $f(\cdot)$ and $f(\cdot \mid y'_i, y_{\text{pa}(i)})$ represent pre-intervention distributions (Pearl, 2009, page 73). The previous expression for $Y_j \notin y_{\text{pa}(i)}$ is a special case of the back-door adjustment (Pearl, 2009, page 79) since $\text{pa}(i)$ satisfies the back-door criterion on (Y_i, Y_j) when $Y_j \notin y_{\text{pa}(i)}$.

2.3 Gaussian DAG-models

If the joint distribution of \mathbf{Y} is Gaussian, we have

$$\mathbf{Y} \sim \mathcal{N}(\boldsymbol{\mu}, \boldsymbol{\Sigma}), \quad (9)$$

where the precision matrix $\boldsymbol{\Omega} = \boldsymbol{\Sigma}^{-1}$ is symmetric, positive definite and Markov relative to \mathcal{G} . By the normality assumption, the Gaussian DAG-model is guaranteed to be faithful to the DAG almost everywhere in the parameter space, implying that the conditional independence relationships entailed by the distribution are exactly the same as those encoded by the DAG via the Markov property (Pearl, 2009, p. 48). For a Gaussian DAG-model, the factorization in Eq. (6) takes the form (see e.g. Geiger and Heckerman (2002))

$$f(y_1, \dots, y_n \mid \mathcal{G}, \boldsymbol{\mu}, \boldsymbol{\Sigma}) = \prod_{m=1}^n \phi(y_m \mid \mu_m(y_{\text{pa}(m)}), \sigma_m^2), \quad (10)$$

where ϕ denotes the univariate normal density function. In this case, Eq. (6) can also be written as a linear structural equation model (SEM)

$$Y_j = \beta_{0j} + \sum_{h \in \text{pa}(Y_j)} \beta_{hj} Y_h + \epsilon_j, \quad \forall j = 1, \dots, n, \quad (11)$$

where the parameters β_{hj} are called the *path coefficients* and the error terms $\epsilon_1, \dots, \epsilon_n$ are mutually independent with mean 0 and finite variance $\mathbf{V} = \text{diag}(\mathbf{v})$, with \mathbf{v} the $(n, 1)$ vector

of variances whose m -th element is $v_m = \text{Var}(\epsilon_m)$. If we assume a topological ordering of the vertices, meaning there exists a label permutation (π_1, \dots, π_n) of the vertices $V = (1, \dots, n)$ such that $(h, j) \in E$ implies $\pi_h < \pi_j$, the matrix $(\mathbf{B}) = \{\beta_{jh}, h \leq j\}$, the transpose of the matrix of path coefficients, is lower-triangular and the covariance matrix $\mathbf{\Sigma}$ is symmetric and positive definite, with the following Cholesky decomposition (Silva and Ghahramani, 2009)

$$\mathbf{\Sigma} = (\mathbf{I} - \mathbf{B})^{-1} \mathbf{V} (\mathbf{I} - \mathbf{B})^{-\top}. \quad (12)$$

By induction on the number of vertices V , one can show that such topological ordering always exists, even if it is not unique in general.

Eq. (11) can be fitted using linear regression and is called structural because it is assumed to hold for the interventional distribution as well with the exception of the intervened upon variable. Given a linear SEM, the total causal effect $\beta(Y_h \rightarrow Y_j)$, of Y_h on Y_j , may be evaluated as the product of the path coefficients along all directed path (causal paths) $\mathcal{C}(h, j)$ from vertex h to j (Wright, 1934).

$$\beta(Y_h \rightarrow Y_j) = \sum_{(k_0, \dots, k_m) \in \mathcal{C}(h, j)} \prod_{l=1}^m \beta_{k_{l-1}k_l} = [(\mathbf{I} - \mathbf{B})^{-\top}]_{hj} \quad (13)$$

It is common to summarize the post-intervention distribution of Eq. (8) by its mean $\mathbb{E}(Y_j \mid \text{do}(Y_i = y'_i))$ and when Y_j is continuous, the total causal effect of $\text{do}(Y_i = y'_i)$ on Y_j is defined as

$$\frac{\partial}{\partial y'_i} \mathbb{E}(Y_j \mid \text{do}(Y_i = y_i)) \Big|_{y_i = y'_i}. \quad (14)$$

Due to the linearity of expectation in the Gaussian case, the mean under the post-intervention distribution in Eq. (8) becomes

$$\mathbb{E}(Y_j \mid y'_i, y_{\text{pa}(i)}) = \lambda_{0j} + \lambda_i y'_i + \sum_{h \in \text{pa}(Y_j)} \lambda_{hj} Y_h. \quad (15)$$

One can show that in this scenario the causal effect of Y_i on Y_j with $Y_j \notin \text{pa}(Y_i)$ corresponds to the regression parameter λ_i associated to the variable Y_i in Eq. (15) (see p. 3138 of Maathuis et al., 2009). For this reason, in the Gaussian case, the causal effect does not depend on the intervention value y'_i and can be interpreted for any value of y'_i as

$$\mathbb{E}(Y_j \mid \text{do}(Y_i = y'_i + 1)) - \mathbb{E}(Y_j \mid \text{do}(Y_i = y'_i)).$$

To model a binary response X_1 potentially affected by a set of observed continuous variables (Y_2, \dots, Y_n) , Castelletti and Consonni (2021) assumed a DAG-Probit model, where the observable binary outcome is obtained by discretizing a continuous latent variable Y_1

$$X_1 = \begin{cases} 1 & \text{if } Y_1 \in [\alpha_1, +\infty) \\ 0 & \text{if } Y_1 \in (-\infty, \alpha_1) \end{cases} \quad \text{for } \alpha_1 \in (-\infty, +\infty) \quad (16)$$

and the joint distribution of (Y_1, \dots, Y_n) is Gaussian and Markov w.r.t. \mathcal{G} as in Eq. (10). In their construction the latent outcome variable is the last one in topological order and therefore it cannot have children.

Under this setting, to determine the effect of an intervention on the observable response variable, one may evaluate

$$\begin{aligned}\mathbb{E}(X_1 \mid \text{do}(Y_i = y'_i), \boldsymbol{\mu}, \boldsymbol{\Sigma}, \alpha_1, \mathcal{G}) &= \mathbb{P}(X_1 = 1 \mid \text{do}(Y_i = y'_i), \boldsymbol{\mu}, \boldsymbol{\Sigma}, \alpha_1, \mathcal{G}) \\ &= \mathbb{P}(Y_1 \geq \alpha_1 \mid \text{do}(Y_i = y'_i), \boldsymbol{\mu}, \boldsymbol{\Sigma}, \mathcal{G}) \\ &= 1 - \Phi\left(\frac{\alpha_1 - \mu_1 - \gamma_i y'_i}{\xi_1^2}\right),\end{aligned}\tag{17}$$

where both γ_i and ξ_1^2 can be expressed in terms of product between submatrices of $\boldsymbol{\Sigma}$, as they are determined by the specialization of the post-interventional distribution in Eq. (8) to the case of the latent Gaussian Y_1 (see Prop. 3.1. of Castelletti and Consonni, 2021).

Similarly to Eq. (14), one may compute

$$\frac{\partial}{\partial y_i} \mathbb{E}(X_1 \mid \text{do}(Y_i = y_i), \boldsymbol{\Sigma}, \theta_0, \mathcal{G}) \Big|_{y_i=y'_i},$$

but this will still depend on y'_i (unlike in the Gaussian continuous case), and the parameters of the DAG Probit model. For this reason, and because Eq. (17) admits an intuitive interpretation as a probability, Castelletti and Consonni (2021) simply denote $\mathbb{P}(X_1 = 1 \mid \text{do}(Y_i = y'_i), \boldsymbol{\mu}, \boldsymbol{\Sigma}, \alpha_1, \mathcal{G})$ as the causal effect on X_1 due to an intervention $\text{do}(Y_i = y'_i)$.

2.4 Latent Gaussian DAG-model

To model ordinal variables, we assume that the variables in the Gaussian vector $\mathbf{Y} = (Y_1, \dots, Y_n)^\top$ are unobserved, and we observe instead ordinal variables obtained from the continuous variables by discretisation. The diagram in Fig. 1 provides a visual representation of the set-up in an illustrative case with a handful of variables. Each ordinal variable X_m is assumed to be a discretised version of the latent variable Y_m . Specifically, given a vector of thresholds $\boldsymbol{\alpha}_m = (-\infty := \alpha(m, 0), \dots, \alpha(m, L_m) := \infty)^\top$

$$X_m = \begin{cases} \tau(m, 1) & \text{if } Y_m \in (-\infty, \alpha(m, 1)) \\ \vdots & \\ \tau(m, L_m) & \text{if } Y_m \in [\alpha(m, L_m - 1), +\infty). \end{cases}\tag{18}$$

Formally, the latent (Gaussian) DAG-model for ordinal variables is defined by

$$\begin{aligned}Y_m \mid \mathbf{y}_{\text{pa}(m)}, \vartheta_m, \mathcal{G} &\sim \mathcal{N}\left(\mu_m + \sum_{j \in \text{pa}(m)} b_{jm}(y_j - \mu_j), v_m\right) \\ \mathbb{P}(X_m = \tau(m, l) \mid Y_m = y_m, \boldsymbol{\alpha}_m) &= \mathbb{1}\left(y_m \in [\alpha(m, l - 1), \alpha(m, l)]\right), \quad l = 1, \dots, L_m\end{aligned}\tag{19}$$

$$p(\mathbf{x}, \mathbf{y} \mid \theta, \mathcal{G}) = \prod_{m=1}^n \phi(y_m \mid \mathbf{y}_{\text{pa}(m)}, \vartheta_m, \mathcal{G}) p(x_m \mid y_m, \boldsymbol{\alpha}_m)$$

where $\theta = \cup_{m=1}^n \theta_m$ with $\theta_m = (\vartheta_m, \boldsymbol{\alpha}_m)$, $\vartheta_m = (\mu_m, \mathbf{b}_m, v_m)$ and $\mathbf{b}_m = (b_{jm})_{j \in \text{pa}(m)}$ for all $m = 1, \dots, n$.

To ensure model identifiability, we require additional constraints. In fact, different hidden Gaussian variables \mathbf{Y} might generate the same contingency table for the ordinal

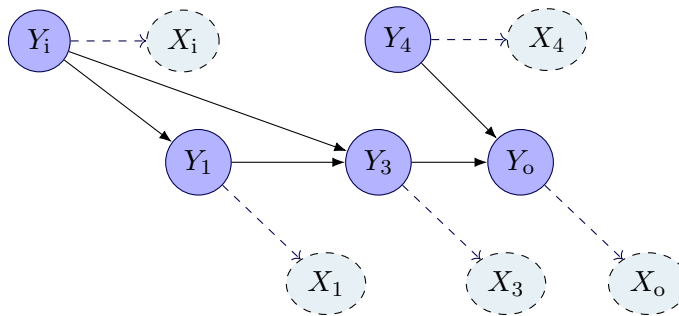


Figure 1: Example of latent Gaussian five-nodes DAG. Variables X_m , $m = 1, \dots, 5$ are ordinal, each obtained by discretizing a latent variable Y_m with associated Gaussian parameters θ_m . Ordinal nodes are dashed for clarity.

variables \mathbf{X} , by shifting and scaling the thresholds according to the corresponding means and variances.

Computationally, the most convenient constraint consists in standardizing each latent dimension, as adopted by Luo et al. (2021), and consists in setting $\mu_m = 0$ for all $m = 1, \dots, n$, $\mathbf{V} = \mathbf{I}$ and replacing the covariance matrix Σ with its correlation form $D^{-1}\Sigma D^{-1}$, where D is a diagonal matrix with elements $d_m = \sqrt{\Sigma_{mm}}$. Nonetheless, in the next section, we derive the causal effects for a generic covariance matrix Σ and mean vector $\boldsymbol{\mu}$ to ensure that the framework remains applicable to the most general case.

3 Causal Effects in the Latent Gaussian DAG Model

Consider the general latent Gaussian DAG-model of Section 2.4 and assume that the parameters θ are given together with the DAG \mathcal{G} . Our interest is in computing the target causal estimand in Eq. (1), representing the OCE on X_o (outcome variable) of an intervention on X_i (intervention variable). Since there is no causal path in the DAG \mathcal{G} between the ordinal X_i and X_o (as in the illustrative graphical representation in Fig. 1), the direct computation of Eq. (1) would lead to 0 for each level of the intervention and outcome variable.

Despite the absence of a causal path between the ordinal variables X_i and X_o , it is evident that they are casually related to each other through their corresponding latent parent variables. Hence, we can consider that if we were to intervene on the latent variable Y_i in a way that changes the level of its ordinal child variable X_i and then compute the effect of this intervention on the latent parent Y_o of X_o , it is possible that the level assumed by X_o would also change as a consequence. The potential change in the level of X_o determined by an intervention on the latent parent of X_i that shifts its level then becomes the effect of interest here. Using the discretising thresholds $\boldsymbol{\alpha} = \cup_{m=1}^n \boldsymbol{\alpha}_m$, the target causal estimand in Eq. (1) on the ordinal variables can be equivalently computed as the following difference in probabilities on the latent scale.

Definition 1 (Ordinal Causal Effect). Let $\mathbf{Y} = (Y_1, \dots, Y_n) \sim \mathcal{N}(\mathbf{0}, \Sigma)$ be the underlying vector of variables in a Latent Gaussian DAG model. Let Y_i , $i \in \{1, \dots, n\}$ be the latent intervention variable and Y_o , $o \in \{1, \dots, n\} \setminus \{i\}$ the latent outcome variable. The Ordinal

Causal Effect (OCE) on Y_o of intervening on Y_i is given by

$$\begin{aligned} \text{OCE}_{i_o}(k, l \rightarrow l') &= \mathbb{P}\left[Y_o \in [\alpha(o, k-1), \alpha(o, k)] \mid \text{do}(Y_i \in [\alpha(i, l'-1), \alpha(i, l')])\right] \\ &\quad - \mathbb{P}\left[Y_o \in [\alpha(o, k-1), \alpha(o, k)] \mid \text{do}(Y_i \in [\alpha(i, l-1), \alpha(i, l)])\right] \end{aligned} \quad (20)$$

for each $1 \leq k \leq L_o$, $1 \leq l, l' \leq L_i$, with $l \neq l'$.

Notice that the definition of OCE is anti-symmetric in the initial and end level of the intervention variable, meaning that

$$\text{OCE}_{i_o}(k, l \rightarrow l') = -\text{OCE}_{i_o}(k, l' \rightarrow l).$$

In Eq. (20), $\text{do}(Y_i \in [\alpha(i, l-1), \alpha(i, l)])$ denotes a deterministic intervention on Y_i , which consists in setting Y_i to a value \tilde{y}_i belonging to the interval $[\alpha(i, l-1), \alpha(i, l)]$. To perform this intervention, we may enforce the atomic intervention $\text{do}(Y_i = \tilde{y}_i)$ with a certain probability distribution $f^*(\tilde{y}_i)$, called the *intervention policy*, which will modify the distribution of Y_i so that the intervention value \tilde{y}_i belongs to the interval of interest as following:

$$f(y_o) \Big|_{f^*(\tilde{y}_i)} = \int_{\mathcal{Y}_i} f(y_o \mid \text{do}(Y_i = \tilde{y}_i)) f^*(\tilde{y}_i) d\tilde{y}_i, \quad (21)$$

where \mathcal{Y}_i represents the support of Y_i under intervention, meaning that f^* is any normalized density over the interval $[\alpha(i, l-1), \alpha(i, l)]$. Given that any distribution of Y_i with support on the previous interval is an eligible intervention policy $f^*(\tilde{y}_i)$, $\text{do}(Y_i \in [\alpha(i, l-1), \alpha(i, l)])$ is not uniquely defined.

Definition 2. Under the same model of Definition 1 and given the two intervention policies $f^*(\tilde{y}_i)$ and $f^{**}(y'_i)$ with support respectively on $[\alpha(i, l-1), \alpha(i, l)]$ and $[\alpha(i, l'-1), \alpha(i, l')]$, the ordinal causal effect in Definition 1 is given by:

$$\begin{aligned} \text{OCE}_{i_o}(k, l \rightarrow l') &= \int_{\alpha(o, k-1)}^{\alpha(o, k)} \int_{\mathcal{Y}'_i} f(y_o \mid \text{do}(Y_i = y'_i)) f^{**}(y'_i) dy'_i dy_o \\ &\quad - \int_{\alpha(o, k-1)}^{\alpha(o, k)} \int_{\tilde{\mathcal{Y}}_i} f(y_o \mid \text{do}(Y_i = \tilde{y}_i)) f^*(\tilde{y}_i) d\tilde{y}_i dy_o, \end{aligned} \quad (22)$$

for each $1 \leq k \leq L_o$, $1 \leq l, l' \leq L_i$, with $l \neq l'$.

In Eq. (22), the atomic post-intervention density of Y_o is analytically identifiable through the truncated factorization formula in Eq. (7), as stated in the following.

Proposition 3. Let $(Y_1, \dots, Y_n) \sim \mathcal{N}(\boldsymbol{\mu}, \boldsymbol{\Sigma})$ and consider the do operator $\text{do}(Y_i = \tilde{y}_i)$, $i \in \{1, \dots, n\}$. Then the atomic post-intervention distribution of Y_o , $o \in \{1, \dots, n\} \setminus \{i\}$ is

$$f(y_o \mid \text{do}(Y_i = \tilde{y}_i), \boldsymbol{\mu}, \boldsymbol{\Sigma}) = \phi(\boldsymbol{\mu}_{\text{do}}, \boldsymbol{\Sigma}_{\text{do}}), \quad (23)$$

where

$$\begin{aligned} a &= \{\text{pa}(i), i\}, & b &= \{o\}, \\ \boldsymbol{\mu}_{\text{do}} &= \boldsymbol{\mu}_o + (\boldsymbol{\Sigma}_{ba} \boldsymbol{\Sigma}_{aa}^{-1})_i (y_i - \mu_i), \\ \boldsymbol{\Sigma}_{\text{do}} &= \boldsymbol{\Sigma}_{bb} - (\boldsymbol{\Sigma}_{ba} \boldsymbol{\Sigma}_{aa}^{-1}) \boldsymbol{\Sigma}_{ab} + (\boldsymbol{\Sigma}_{ba} \boldsymbol{\Sigma}_{aa}^{-1})_{-i} \boldsymbol{\Sigma}_{\text{pa}(i)\text{pa}(i)} (\boldsymbol{\Sigma}_{ba} \boldsymbol{\Sigma}_{aa}^{-1})_{-i}^\top. \end{aligned} \quad (24)$$

Proof. See Appendix A.2. ■

The previous proposition is equivalent to Prop. 3.1. of Castelletti and Consonni (2021), as we also consider a collection of jointly Gaussian variables described by a DAG. Since the latent Gaussian DAG-model is not miss-specified, for each admissible adjustment set, the atomic post-intervention distribution would result in a normal with parameters μ_{do} and Σ_{do} depending only on intervention and outcome variables. The proposition below provides a simplified version of the previous result, incorporating the intervention model.

Proposition 4. *Let $(Y_1, \dots, Y_n) \sim \mathcal{N}(\boldsymbol{\mu}, \boldsymbol{\Sigma})$, with $\boldsymbol{\Sigma} = (\mathbf{I} - \mathbf{B})^{-1} \mathbf{V} (\mathbf{I} - \mathbf{B})^{-\top}$ as in Eq. (12). Consider the do operator $\text{do}(Y_i = \tilde{y}_i)$, $i \in \{1, \dots, n\}$. Then the post-intervention distribution of Y_o , $o \in \{1, \dots, n\} \setminus \{i\}$ is*

$$f(y_o \mid \text{do}(Y_i = \tilde{y}_i), \boldsymbol{\Sigma}) = \phi(\tilde{\boldsymbol{\mu}}_o, \tilde{\boldsymbol{\Sigma}}_{oo}), \quad (25)$$

with

$$\tilde{\boldsymbol{\mu}}_o = \boldsymbol{\mu}_o + \mathbf{W}_{oi} (y_i - \mu_i), \quad \tilde{\boldsymbol{\Sigma}}_{oo} = \left[(\mathbf{I} - \tilde{\mathbf{B}})^{-1} \tilde{\mathbf{V}} (\mathbf{I} - \tilde{\mathbf{B}})^{-\top} \right]_{oo}, \quad (26)$$

where

$$\begin{aligned} \mathbf{W} &= (\mathbf{I} - \mathbf{B})^{-1} \\ \tilde{\mathbf{V}} &= \text{diag}(v_1, \dots, v_{i-1}, 0, v_{i+1}, \dots, v_n) \\ \tilde{\mathbf{B}}_{hj} &= \begin{cases} 0 & \text{if } j = i \\ \mathbf{B}_{hj} & \text{otherwise} \end{cases} \end{aligned} \quad (27)$$

Proof. See Appendix A.3. ■

The result in the proposition is independent of the chosen adjustment set: in general, to compute Σ_{do} of Eq. (24), it is sufficient to consider the variables preceding the outcome in topological order, and for each of these variables Y_j , add the contribution to the variance of the outcome variable along those paths, from Y_j to the outcome, that do not intercept the intervention variable. Proposition 4 offers a fast and efficient method for determining the parameters of the post-intervention distribution, and aligns with the interpretation of interventions in the latent space.

Once the atomic post-intervention distribution $f(y_o \mid \text{do}(Y_i = \tilde{y}_i))$ is determined through Proposition 4, we need to select proper intervention policies $f^*(\tilde{y}_i)$ and $f^{**}(y'_i)$ to compute the ordinal causal effect through Eq. (22). Below we cover two slightly different conceptual strategies.

One option is to shift the value of the latent variable \tilde{y}_i to any point $y'_i \in [\alpha(i, l' - 1), \alpha(i, l')]$, by choosing the same distribution family for both intervention policies, and hereafter we refer to this as the distributional approach. Alternatively, we may define the intervention in the latent space, so that y'_i is the corresponding point (in *quantile-sense*) to the point \tilde{y}_i , i.e.

$$F^* \left[Y_i \leq \tilde{y}_i \right] = F^{**} \left[Y_i \leq y'_i \right], \quad (28)$$

and therefore y'_i is a function of \tilde{y}_i

$$y'_i = F^{**^{-1}}(F^*(\tilde{y}_i)). \quad (29)$$

Henceforth we refer to the latter strategy as the quantile approach.

The two approaches turn out to be equivalent for the computation of OCE when choosing truncated normals as intervention policies, see Appendix A.5. The quantile approach extends easily to different choices of intervention policy, though the equivalence with the distributional approach might no longer hold.

The following proposition provides a closed formula to compute OCE in the general case when using a distributional approach and the truncated normal distribution as intervention policy, which seems the most natural choice given that the marginal and the pre-intervention distribution of Y_i is normal.

Proposition 5 (Computation of the Ordinal Causal Effect).

$$\begin{aligned} & \text{OCE}_{\text{io}}(k, l \rightarrow l') \\ &= \frac{1}{\Phi(\bar{\alpha}(i, l')) - \Phi(\bar{\alpha}(i, l' - 1))} \begin{bmatrix} \mathcal{BN}(\bar{\alpha}(i, l'), \tilde{a}_k, \rho) & -\mathcal{BN}(\bar{\alpha}(i, l' - 1), \tilde{a}_k, \rho) \\ -\mathcal{BN}(\bar{\alpha}(i, l'), \tilde{a}_{k-1}, \rho) & +\mathcal{BN}(\bar{\alpha}(i, l' - 1), \tilde{a}_{k-1}, \rho) \end{bmatrix} \end{aligned} \quad (30)$$

$$- \frac{1}{\Phi(\bar{\alpha}(i, l)) - \Phi(\bar{\alpha}(i, l - 1))} \begin{bmatrix} \mathcal{BN}(\bar{\alpha}(i, l), \tilde{a}_k, \rho) & -\mathcal{BN}(\bar{\alpha}(i, l - 1), \tilde{a}_k, \rho) \\ -\mathcal{BN}(\bar{\alpha}(i, l), \tilde{a}_{k-1}, \rho) & +\mathcal{BN}(\bar{\alpha}(i, l - 1), \tilde{a}_{k-1}, \rho) \end{bmatrix}. \quad (31)$$

where Φ and \mathcal{BN} are respectively the c.d.f. of a standard normal distribution and the p.d.f. of a standard bivariate normal distribution and

$$\begin{aligned} \bar{\alpha}(i, l) &= \frac{\alpha(i, l) - \mu_i}{\sigma_i} \quad \forall 1 \leq l \leq L_i \quad \text{with } \sigma_i = \sqrt{\Sigma_{ii}}; \\ \bar{\alpha}(o, k) &= \frac{\alpha(o, k) - \tilde{\mu}_o}{\sqrt{\tilde{\Sigma}_{oo}}} = \frac{\alpha(o, k) - \mu_o}{\sqrt{\tilde{\Sigma}_{oo}}} - \frac{\mathbf{W}_{oi}\sigma_i}{\sqrt{\tilde{\Sigma}_{oo}}} z_i = a_k + bz_i, \forall 1 \leq k \leq L_o, \text{ with } z_i = \frac{\tilde{y}_i - \mu_i}{\sigma_i}; \\ \tilde{a}_k &= \frac{a_k}{\sqrt{1+b^2}}, \quad \rho = -\frac{b}{\sqrt{1+b^2}}. \end{aligned} \quad (32)$$

Proof. See Appendix A.4. ■

Note that Eq. (30) and Eq. (31) can also be expressed using Owen's T function (Owen, 1980, formula 3.1). Furthermore, for a binary intervention variable, Proposition 5 can be applied to recover the distributional causal effects of Eq. (2).

In the special case of two binary variables, we verified in Appendix B.1 that our method for computing causal effects produces results in agreement with the causal risk differences. However, this equivalence breaks down already for three binary variables due to the limitations of the latent Gaussian construction in fully representing their distribution, as detailed in Appendix B.2.

4 Experimental Results

In this section, we present simulation studies where we evaluate the performance of our proposed method in estimating ordinal effects for both, known and unknown latent network structures. Finally, we show a real-world application to a psychological dataset (McNally et al., 2017) combining information about obsessive-compulsive disorder and co-morbid depression symptoms.

For the simulations and analysis, we adopted R statistical software (R Core Team, 2023, v.4.4.1) to implement the computational approach for the formula in Proposition 5. Details of the different implementation methods and comparisons are provided in Appendix B.3.

4.1 Simulations

In our simulation study, we generate a random Erdős–Rényi graph DAG with 16 nodes using the `randDAG` function from the `pcalg` package (Kalisch et al., 2012), where each node is expected to have 5 neighbours, and illustrated in Appendix B.3. We explicitly chose a DAG which is the only element of its Markov equivalence class. The edge weights are sampled uniformly from the intervals $(-1, -0.4)$ and $(0.4, 1)$. Next, we generate the corresponding Gaussian sample $\mathcal{D}_{\mathbf{Y}} = \{\mathbf{y}^1, \dots, \mathbf{y}^N\}$ for the latent variable \mathbf{Y} with a sample size of $N = 500$ following the topological order in the DAGs. To ensure identifiability, as already discussed in Section 2.4, we standardized each variable of the Gaussian dataset, centring it at its mean and transforming its covariance matrix into the correlation form. Lastly, we convert the Gaussian sample into an ordinal sample $\mathcal{D}_{\mathbf{X}} = \{\mathbf{x}^1, \dots, \mathbf{x}^N\}$ of size N for the ordinal variables \mathbf{X} . To this aim, each continuous underlined Gaussian variable Y_m is randomly discretised into ordinal levels through a series of thresholds α_m , which are generated through the symmetric Dirichlet distribution $\text{Dir}(L_m, \nu)$, where L_m denotes the number of expected ordinal levels for variable X_m , and ν is the concentration parameter. In our simulations, L_m is randomly chosen from the set $[2, 6]$ to get 4 expected number of levels for each variable, and we set $\nu = 2$ to prevent levels with very small probabilities. Specifically, the cell probabilities for the ordinal contingency tables of X_m are first derived using $\text{Dir}(L_m, \nu)$, and based on these probabilities, we calculate the thresholds for cutting the Gaussian variable in dimension m using the normal quantile function.

We regenerate 500 times the Gaussian dataset $\mathcal{D}_{\mathbf{Y}}$ and we cut each of the regenerated datasets according to the original cuts to obtain the corresponding ordinal sample. Furthermore, to gain insights into the variability of plausible causal effects from a given dataset, we implement a non-parametric bootstrap procedure resampling with replacement from the ordinal dataset $\mathcal{D}_{\mathbf{X}}$ to obtain $M = 500$ bootstrapped datasets, while maintaining the sample size $N = 500$. For both procedures, we compare the estimates of the causal effects to the theoretical estimates from the known graph and parameters, under two different scenarios, named ‘Param’ and ‘BN’ respectively:

Param: for the known DAG \mathcal{G} , use OSEM (Luo et al., 2021) to only learn the discretisation thresholds α^j and the parameters $\vartheta^j = \cup_{m=1}^n \vartheta_m^j$ for each $j = 1, \dots, M$;

BN: for unknown graphical structures, use OSEM to learn both thresholds $\alpha^j = \cup_{m=1}^n \alpha_m^j$ and the Bayesian Network $\mathcal{B}^j = (\mathcal{G}^j, \vartheta^j = \cup_{m=1}^n \vartheta_m^j)$ for each $j = 1, \dots, M$.

In both cases we employ the learned thresholds, parameters and either given or learned structure to compute the OCEs.

As an example of comparison of our methodology’s performance under the two scenarios, in Fig. 2 for the simulation with regenerated data and in Fig. 3 for bootstrapped ones, we report the OCEs resulting from shifting variable 1 from its lowest to its upper level on all the other variables through Raincloud plots (Allen et al., 2021) compared with the true effects determined through the original ordinal dataset. Analogous plots for the other roots nodes in the True DAG (i.e. 8,11,15) are available in Appendix B.3. For each pair of intervention and outcome variables among the 16 nodes in the DAG, similar plots are available online (see Section 6).

As expected, when the graph structure is already known (‘Param’ approach), our methodology demonstrates improved compatibility in recovering causal effects compared to the ‘BN’ approach, where additional uncertainty about the graph structure is introduced. In both scenarios and simulations, the estimates of OCEs depend on the quality of approximation of the underlying covariance matrix, which is obtained through the Monte Carlo EM Algorithm (Wei and Tanner, 1990) in OSEM (Luo et al., 2021). With increasing sample size, the contingency tables become more reliable, so recovering the original covariance structure through the EM iterations should become more accurate.

Overall, the mean causal effects across the two approaches remain largely compatible with the theoretical values, as evidenced by the regenerated data simulation, where the distribution of effects is generally centred on the true effects. Deviations from this pattern, such as in outcome variable 3, can be attributed to deviations in the estimation of the underlying correlation matrix when using the default settings of OSEM. This is particularly the case when these are compounded through paths in the network, as in the case of variable 9, which is a descendant of variable 1 only through variable 3. Improving the accuracy of correlation matrix estimation could therefore enhance the overall reliability of causal effect estimation within our framework.

4.2 Analysis of Psychological Data

In this section, we apply our method to psychological survey data, where preserving the ordinal structure might be particularly valuable for accurately estimating causal effects. We use an ordinal dataset comprising data about 408 adults from McNally et al. (2017) study on the functional relationships between 10 five-level symptoms of obsessive-compulsive disorder (OCD) and 16 four-level depression symptoms (McNally et al., 2017), measured with the self-report Yale-Brown Obsessive-Compulsive Scale (Y-BOCS-SR) (Steketee et al., 1996) and the Quick Inventory of Depressive Symptomatology (QIDS-SR) (Rush et al., 2003) respectively. Because two pairs of variables in the original depression dataset fundamentally encode the same information, we followed the approach in Luo et al. (2021) to combine each pair in a single variable with seven levels. Details of the symptoms included in the latent DAG-model are summarised in Supplementary Table S2 of Luo et al. (2021).

We followed the procedure in Luo et al. (2021) to obtain DAG estimates from 500 bootstrap samples of the data by running the OSEM algorithm with Monte Carlo sample size $K = 5$ and penalty coefficient $\lambda = 6$.

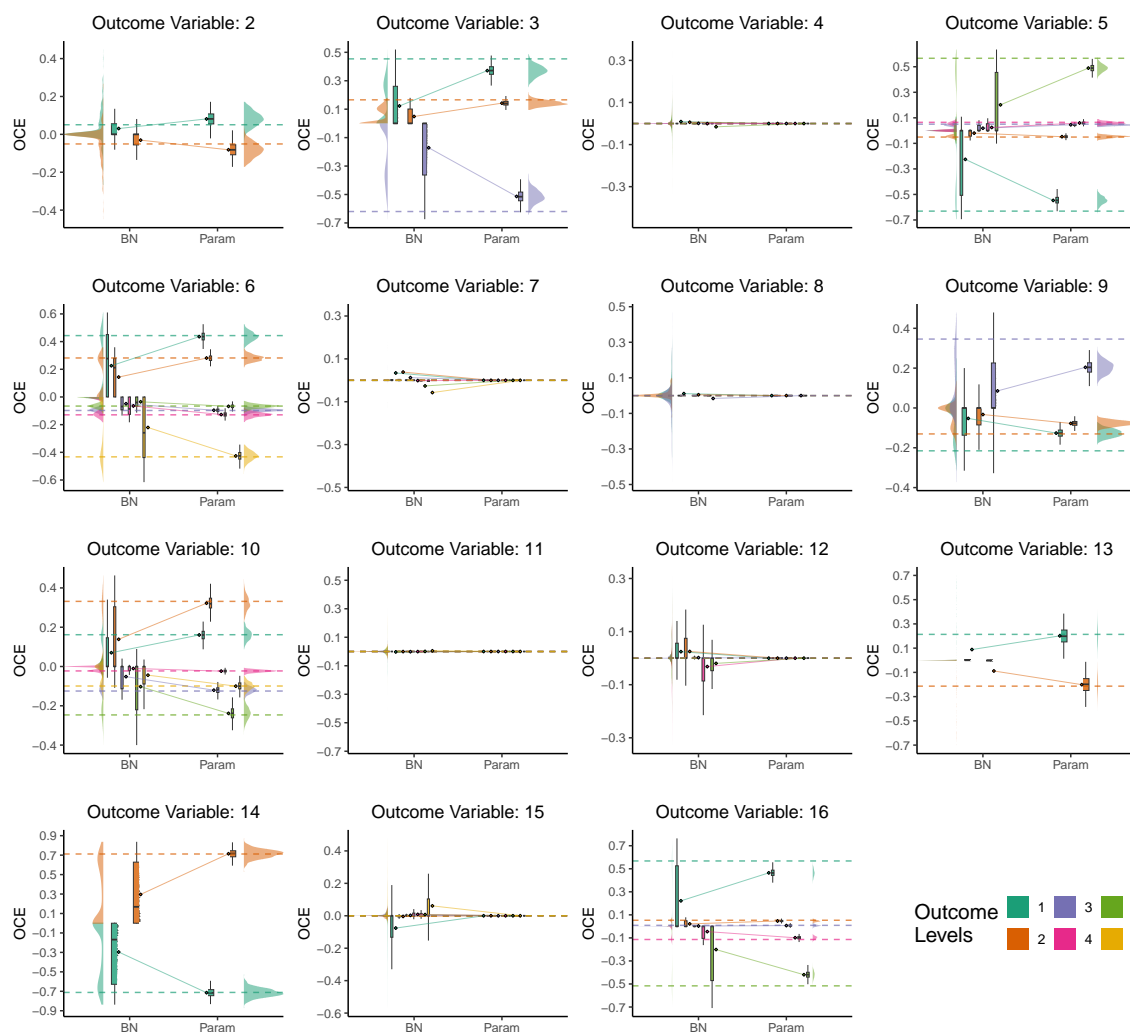


Figure 2: Simulation with Regenerated Data: Ordinal Causal Effects resulting from shifting the intervention variable 1 from its lowest to its upper level on all other outcome variables. For each level of the outcome, the solid line connects the means of the OCEs (represented by diamond points) across different scenarios, while the dotted line represents the True Causal Effect.

As a visual representation of the bootstrapped estimates, we display the adjacency matrices of the DAGs obtained via OSEM converted to CPDAGs in a heatmap in Fig. 15 of Appendix B.3, where the intensity of each cell is proportional to how often each edge appears in the bootstrapped sample. Further, we investigate the causal relationship along the direct edge most frequently appearing in the 500 bootstrapped CPDAGs, by deriving the ordinal causal direct effects of anhedonia (variable 9) on fatigue (variable 10) in the

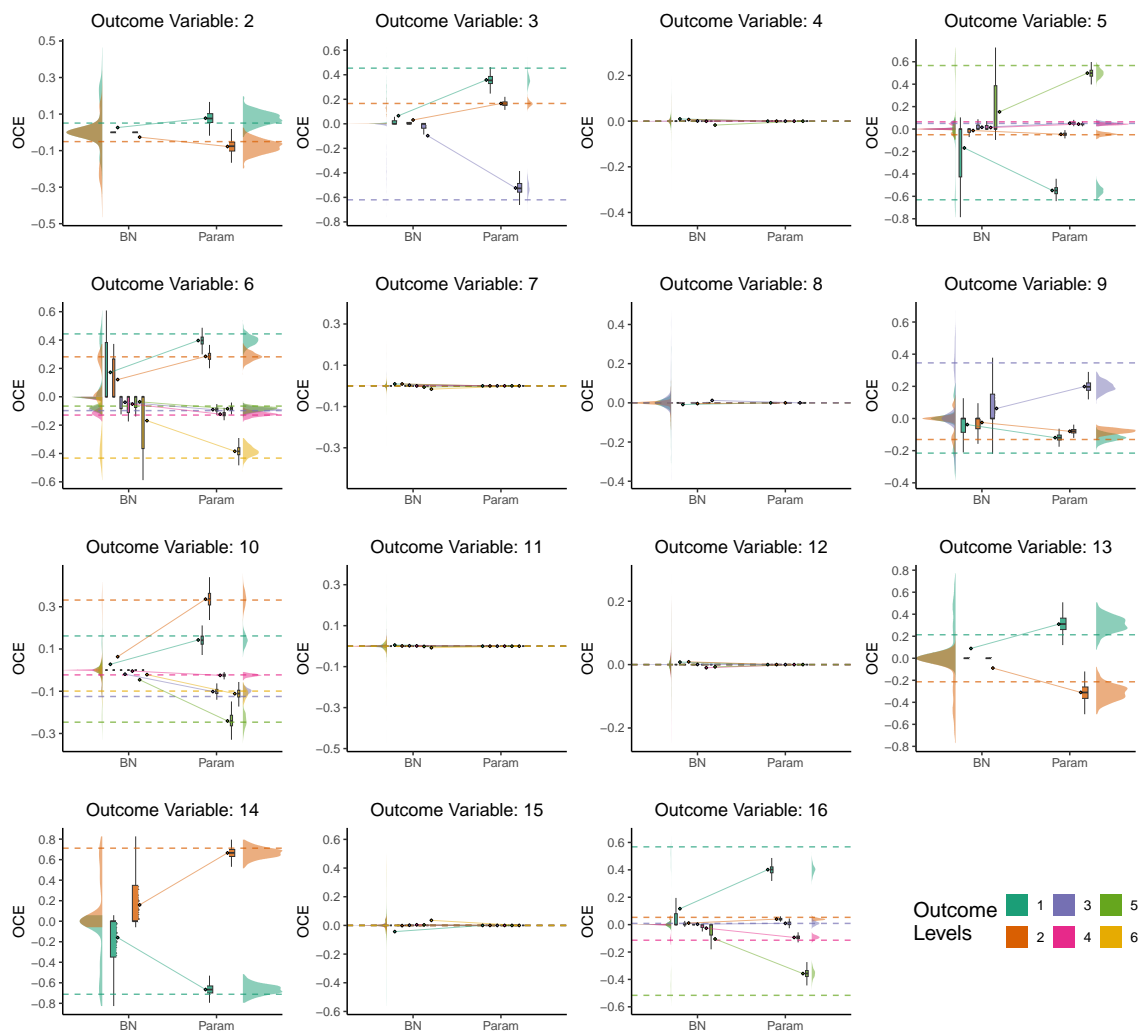


Figure 3: Simulation with Bootstrapped Data: Ordinal Causal Effects resulting from shifting the intervention variable 1 from its lowest to its upper level on all other outcome variables. For each level of the outcome, the solid line connects the means of the OCEs (represented by diamond points) across different scenarios, while the dotted line represents the True Causal Effect.

DAGs in the sample. Raincloud plots including histograms and boxplots of the estimated effects appear in Fig. 4. Finally, we also display raincloud plots summarising the effects of shifting variable 9 from its lowest to its upper level on all other variables and for all their levels in Fig. 16 of Appendix. Analogous plots for all other possible choices of intervention variables are available online (see Section 6).

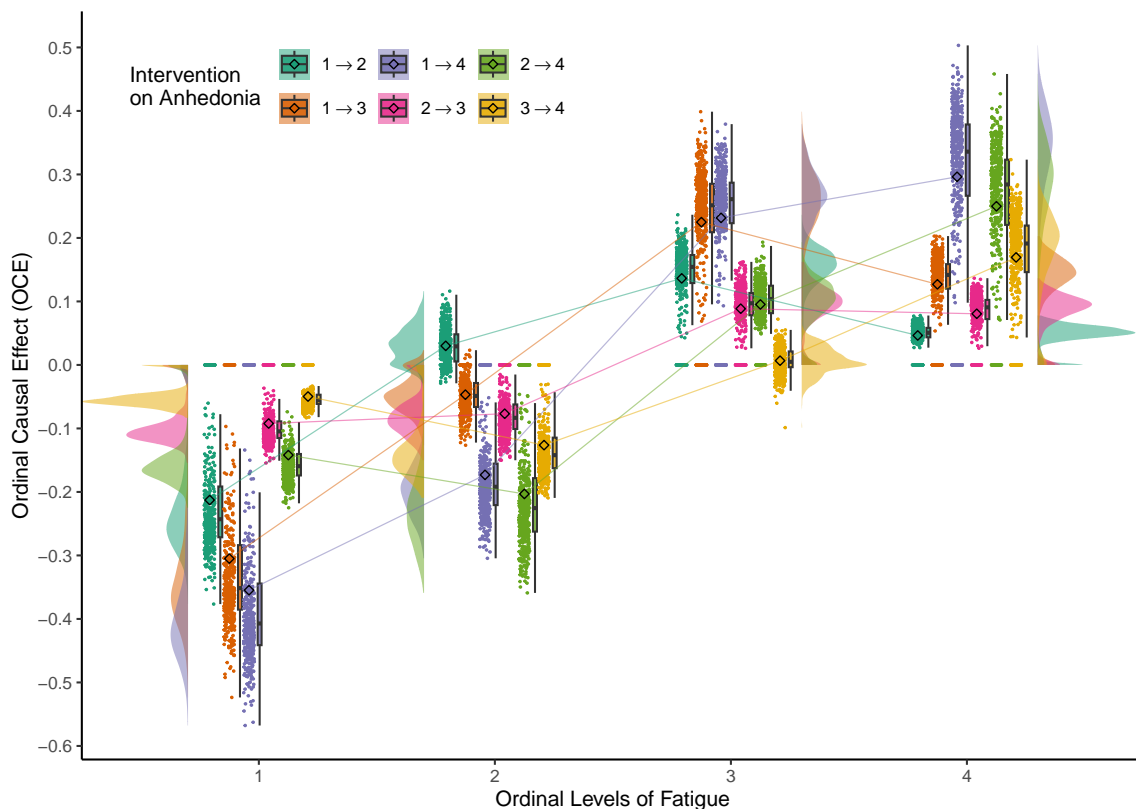


Figure 4: Ordinal Causal Effect of Anhedonia (variable 9) on Fatigue (variable 10). The solid line connects the means of the OCEs (represented by diamond points) across different levels of the outcome variable, for each possible shift of the intervention variable.

5 Discussion

In this work, we address the challenge of defining and estimating causal effects from ordinal data within a latent Gaussian DAG framework. Modelling each ordinal variable as a marginal discretization of an underlying Gaussian variable has the appeal of preserving the ordinality among categories. Additionally, the construction via a latent continuous multivariate Gaussian distribution enables us to propose a definition of Ordinal Causal Effects starting from pointwise intervention distributions in the latent space. From there we could then derive closed-form expressions for OCEs.

In the special case of two binary variables, our approach reduces to classical methods for estimating causal effects. Our framework also incorporates the causal estimand presented by Lu et al. (2018) which is defined as the shift in the probability of falling above a certain category under a binary treatment. This estimand can be readily derived within our frame-

work by simply adjusting the outer limits of integration in Eq. (22), while our approach can further be employed to estimate the effect with our latent Gaussian framework.

Given the marginal normality of latent variables, we adopt the most natural choice of intervention policy, selecting a truncated normal distribution supported by the band representing the level of the ordinal variable corresponding to the intervention. Although one could use other bounded distributions (such as the uniform distribution), the truncated normal distribution is in line with the latent Gaussian model. Unlike general bounded policies, which work best for inner intervention levels, but struggle to adequately describe interventions targeting semi-infinite intervals like $(-\infty, a)$ or $(b, +\infty)$ with $a, b \in \mathbb{R}$, the truncated normal policy remains well-suited even for intervention targeting first and last levels.

In our simulation studies, we estimated the parameters of a Bayesian network, starting either from a known or an estimated graph structure, using OSEM. Then we could compute the OCEs and compare them with those derived from the true underlying parameters. We further demonstrated the applicability of our methodology by analysing psychological survey data and computed OCEs are computed for a set of bootstrapped DAGs.

Learned DAGs may belong to various Markov equivalence classes, while different DAGs within the same equivalence class may yield distinct causal effects due to variations in the parent sets of the intervened node. For each DAG and its equivalence class, one previous approach (Maathuis et al., 2009) has been to estimate causal effects under each DAG in the equivalence class. However, since exhaustively enumerating all DAGs within a CPDAG can be computationally prohibitive, even for small networks, one can focus on the distinct causal effects within a CPDAG (Maathuis et al., 2009). Alternatively, a Bayesian approach can be employed to sample Bayesian networks (Moffa et al., 2017; Kuipers et al., 2022). This approach automatically accounts for uncertainty in the DAG structure and provides an average over the Markov equivalence classes. For ordinal variables, networks can be sampled following the recent methods proposed by Grzegorzczak (2024). Causal effects can then be estimated using our methodology for each DAG to obtain the posterior distribution of causal effects.

In this work we considered interventions on a single node. However, in practice, an exogenous intervention may simultaneously affect multiple variables, calling for predictions of joint intervention effects on the outcome variable. With our latent Gaussian model, accounting for joint interventions, akin to Nandy et al. (2017), is a natural extension in the latent space. Our approach would then offer the framework to map this to ordinal interventions.

Finally, our methodology could extend to estimating causal effects in mixed data settings, where both continuous and ordinal variables are present. This setting can be modelled as a DAG-based Gaussian structure, with some variables discretized and others remaining continuous. While dealing with mixed continuous and nominal categorical variables would require further extension of the OSEM algorithm for estimating graphical structures and parameters, our framework could form the basis for mapping from the latent to the observed space, and hence for estimating causal effects.

6 Software and Supplementary Materials

Software in the form of R code, together with additional simulations results and complete documentation is available at <https://github.com/martinascauda/OrdinalEffects>.

Acknowledgments and Disclosure of Funding

The authors thank Dr. Enrico Giudice and Dr. Ching Wong for helpful discussions and the University of Basel for hosting Martina Scauda during her Master’s Thesis, funded by the Swiss-European Mobility Program.

References

- A. Agresti. *Analysis of Ordinal Categorical Data*. Wiley Series in Probability and Statistics. John Wiley & Sons, Inc., Hoboken, NJ, USA, 2010.
- A. Agresti and M. Kateri. Ordinal probability effect measures for group comparisons in multinomial cumulative link models. *Biometrics*, 73:214–219, 2017.
- J. H. Albert and S. Chib. Bayesian analysis of binary and polychotomous response data. *Journal of the American Statistical Association*, 88:669–679, 1993.
- M. Allen, D. Poggiali, K. Whitaker, T. R. Marshall, J. van Langen, and R. A. Kievit. Raincloud plots: a multi-platform tool for robust data visualization. *Wellcome Open Research*, 4:63, 2021.
- S. Boes. Nonparametric analysis of treatment effects in ordered response models. *Empirical Economics*, 44:81–109, 2013.
- F. Castelletti. Learning Bayesian networks: a copula approach for mixed-type data. *arXiv preprint*, arXiv:2312.13168, 2023.
- F. Castelletti and G. Consonni. Bayesian causal inference in probit graphical models. *Bayesian Analysis*, 16:1113–1137, 2021.
- Y. Chiba. Bayesian inference of causal effects for an ordinal outcome in randomized trials. *Journal of Causal Inference*, 6:20170019, 2018.
- I. Díaz, E. Colantuoni, and M. Rosenblum. Enhanced precision in the analysis of randomized trials with ordinal outcomes. *Biometrics*, 72:422–431, 2016.
- D. Geiger and D. Heckerman. Parameter priors for directed acyclic graphical models and the characterization of several probability distributions. *The Annals of Statistics*, 30:1412–1440, 2002.
- A. Genz and F. Bretz. *Computation of Multivariate Normal and t Probabilities*. Lecture Notes in Statistics. Springer-Verlag, Heidelberg, 2009.

- M. Grzegorzcyk. Being Bayesian about learning Bayesian networks from ordinal data. *International Journal of Approximate Reasoning*, 170:109205, 2024.
- N. J. Higham. *Accuracy and Stability of Numerical Algorithms*. Society for Industrial and Applied Mathematics, second edition, 2002.
- P. W. Holland. Causal inference, path analysis and recursive structural equations models. *ETS Research Report Series*, 1988:i–50, 1988.
- K. Imai and D. A. Van Dyk. Causal inference with general treatment regimes: Generalizing the propensity score. *Journal of the American Statistical Association*, 99:854–866, 2004.
- G. Imbens. The role of the propensity score in estimating dose-response functions. *Biometrika*, 87:706–710, 2000.
- G. W. Imbens and D. B. Rubin. *Causal Inference for Statistics, Social, and Biomedical Sciences: An Introduction*. Cambridge University Press, 2015.
- M. M. Joffe and P. R. Rosenbaum. Invited commentary: Propensity scores. *American Journal of Epidemiology*, 150:327–333, 1999.
- C. Ju and Z. Geng. Criteria for surrogate end points based on causal distributions. *Journal of the Royal Statistical Society: Series B*, 72:129–142, 2010.
- M. Kalisch, M. Mächler, D. Colombo, M. H. Maathuis, and P. Bühlmann. Causal inference using graphical models with the R package pcalg. *Journal of Statistical Software*, 47:1–26, 2012.
- N. K. Kitson, A. C. Constantinou, Z. Guo, Y. Liu, and K. Chobtham. A survey of Bayesian network structure learning. *Artificial Intelligence Review*, 56:8721–8814, 2023.
- J. Kuipers, G. Moffa, E. Kuipers, D. Freeman, and P. Bebbington. Links between psychotic and neurotic symptoms in the general population: an analysis of longitudinal British national survey data using directed acyclic graphs. *Psychological Medicine*, 49:388–395, 2019.
- J. Kuipers, P. Suter, and G. Moffa. Efficient sampling and structure learning of Bayesian networks. *Journal of Computational and Graphical Statistics*, 31:639–650, 2022.
- S. Laurent. *OwenQ: Owen Q-Function*, 2023. R package version 1.0.7.
- S. Lauritzen. *Graphical Models*. Oxford Statistical Science Series. Clarendon Press, 1996.
- J. Lu, P. Ding, and T. Dasgupta. Treatment effects on ordinal outcomes: Causal estimands and sharp bounds. *Journal of Educational and Behavioral Statistics*, 43:540–567, 2018.
- J. Lu, Y. Zhang, and P. Ding. Sharp bounds on the relative treatment effect for ordinal outcomes. *Biometrics*, 76:664–669, 2020.
- X. G. Luo, G. Moffa, and J. Kuipers. Learning Bayesian networks from ordinal data. *Journal of Machine Learning Research*, 22:1–44, 2021.

- M. H. Maathuis, M. Kalisch, and P. Bühlmann. Estimating high-dimensional intervention effects from observational data. *The Annals of Statistics*, 37:3133–3164, 2009.
- C. Manski. *Partial Identification of Probability Distributions*. Springer Series in Statistics. Springer-Verlag, New York, 2003.
- R. J. McNally, P. Mair, B. L. Mugno, and B. C. Riemann. Co-morbid obsessive-compulsive disorder and depression: a Bayesian network approach. *Psychological Medicine*, 47:1204–1214, 2017.
- G. Moffa, G. Catone, J. Kuipers, E. Kuipers, D. Freeman, S. Marwaha, B. R. Lennox, M. R. Broome, and P. Bebbington. Using directed acyclic graphs in epidemiological research in psychosis: An analysis of the role of bullying in psychosis. *Schizophrenia Bulletin*, 43:1273–1279, 2017.
- P. Nandy, M. H. Maathuis, and T. S. Richardson. Estimating the effect of joint interventions from observational data in sparse high-dimensional settings. *The Annals of Statistics*, 45:647–674, 2017.
- D. B. Owen. A table of normal integrals. *Communications in Statistics - Simulation and Computation*, 9:389–419, 1980.
- J. Pearl. *Causality*. Cambridge University Press, 2nd edition, 2009.
- R Core Team. *R: A Language and Environment for Statistical Computing*. R Foundation for Statistical Computing, Vienna, Austria, 2023.
- F. L. Rios, G. Moffa, and J. Kuipers. Benchpress: A scalable and versatile workflow for benchmarking structure learning algorithms. *arXiv preprint*, arXiv:2107.03863, 2021.
- P. R. Rosenbaum. Effects attributable to treatment: Inference in experiments and observational studies with a discrete pivot. *Biometrika*, 88:219–231, 2001.
- P. R. Rosenbaum and D. B. Rubin. Assessing sensitivity to an unobserved binary covariate in an observational study with binary outcome. *Journal of the Royal Statistical Society: Series B*, 45:212–218, 1983.
- D. B. Rubin. Estimating causal effects of treatments in randomized and nonrandomized studies. *Journal of Educational Psychology*, 66:688–701, 1974.
- A. Rush, M. H. Trivedi, H. M. Ibrahim, T. J. Carmody, B. Arnow, D. N. Klein, J. C. Markowitz, P. T. Ninan, S. Kornstein, R. Manber, M. E. Thase, J. H. Kocsis, and M. B. Keller. The 16-item quick inventory of depressive symptomatology (QIDS), clinician rating (QIDS-C), and self-report (QIDS-SR): a psychometric evaluation in patients with chronic major depression. *Biological Psychiatry*, 54:573–583, 2003.
- R. Silva and Z. Ghahramani. The hidden life of latent variables: Bayesian learning with mixed graph models. *Journal of Machine Learning Research*, 10:1187–1238, 2009.

- J. Splawa-Neyman, D. M. Dabrowska, and T. P. Speed. On the application of probability theory to agricultural experiments. Essay on principles. Section 9. *Statistical Science*, 5: 465–472, 1923.
- G. Steketee, R. Frost, and K. Bogart. The Yale-Brown obsessive compulsive scale: Interview versus self-report. *Behaviour Research and Therapy*, 34:675–684, 1996.
- T. Verma and J. Pearl. Equivalence and synthesis of causal models. In *Proceedings of the Sixth Annual Conference on Uncertainty in Artificial Intelligence*, UAI '90, pages 255–270, 1990.
- J. Viinikka, A. Hyttinen, J. Pensar, and M. Koivisto. Towards scalable Bayesian learning of causal DAGs. In *Advances in Neural Information Processing Systems*, volume 33, pages 6584–6594, 2020.
- A. Volfovsky, E. M. Airoidi, and D. B. Rubin. Causal inference for ordinal outcomes. *arXiv preprint*, arXiv:1501.01234, 2015.
- G. C. G. Wei and M. A. Tanner. A Monte Carlo implementation of the EM algorithm and the poor man's data augmentation algorithms. *Journal of the American Statistical Association*, 85:699–704, 1990.
- S. Wright. The method of path coefficients. *The Annals of Mathematical Statistics*, 5: 161–215, 1934.

Appendix A. Additional Theoretical Results

A.1 A Toy Model

For illustrative purposes, we first provide a definition of causal effect of an intervention in a toy Gaussian DAG-model, where there are just two binary variables X_1 and X_2 , assumed to be obtained by marginally discretizing two underlying Gaussian variables Y_1 and Y_2 . Let the parameters θ and α of the model be given together with the DAG \mathcal{G} , illustrated in Fig. 5.

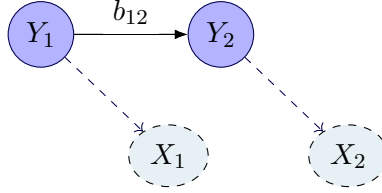


Figure 5: Toy model on DAG \mathcal{G} .

A measure of the causal effect on X_2 of an intervention on X_1 may be the following

$$\mathbb{P}[X_2 = \tau(2, k) \mid \text{do}(X_1 = \tau(1, l'))] - \mathbb{P}[X_2 = \tau(2, k) \mid \text{do}(X_1 = \tau(1, l))] \quad (33)$$

for each $l \neq l'$ and $l, l', k \in \{1, 2\}$. Following Definition 1, Eq. (33) can be equivalently expressed on the latent scale as

$$\begin{aligned} & \mathbb{P}\left[Y_2 \in [\alpha(2, k - 1), \alpha(2, k)] \mid \text{do}(Y_1 \in [\alpha(1, l' - 1), \alpha(1, l')])\right] \\ & - \mathbb{P}\left[Y_2 \in [\alpha(2, k - 1), \alpha(2, k)] \mid \text{do}(Y_1 \in [\alpha(1, l - 1), \alpha(1, l)])\right] \end{aligned} \quad (34)$$

A closed formula to compute it, using either distributional or quantile approach, is provided in Appendix A.5.

A.2 Proof of Proposition 3

Proof. Let

$$\mathbf{Y}_a = \left[\frac{\mathbf{pa}(i)}{Y_i} \right] \quad \text{and} \quad Y_b = [Y_o]$$

be marginally distributed as $(\mathbf{Y}_a, Y_b) \sim \mathcal{N}(\bar{\boldsymbol{\mu}}, \bar{\boldsymbol{\Sigma}})$ with block-wise mean and covariance defined as

$$\bar{\boldsymbol{\mu}} = \begin{bmatrix} \boldsymbol{\mu}_a \\ \mu_b \end{bmatrix} \quad \bar{\boldsymbol{\Sigma}} = \begin{bmatrix} \boldsymbol{\Sigma}_{aa} & \boldsymbol{\Sigma}_{ab} \\ \boldsymbol{\Sigma}_{ba} & \Sigma_{bb} \end{bmatrix}$$

and $|\boldsymbol{\Sigma}_{aa}| > 0$. It follows from classic results on conditional normal distribution that $Y_b \mid \mathbf{Y}_a = \mathbf{y}_a \sim \mathcal{N}(\mu_{b|a}, \Sigma_{b|a})$ is a univariate distribution with

$$\begin{aligned} \mu_{b|a} &= \mu_b + \boldsymbol{\Sigma}_{ba} \boldsymbol{\Sigma}_{aa}^{-1} (\mathbf{y}_a - \boldsymbol{\mu}_a) \\ \Sigma_{b|a} &= \Sigma_{bb} - (\boldsymbol{\Sigma}_{ba} \boldsymbol{\Sigma}_{aa}^{-1}) \boldsymbol{\Sigma}_{ab}. \end{aligned}$$

Here Σ_{aa}^{-1} is the generalized inverse of Σ_{aa} and $\Sigma_{b|a}$ is the Shur complement of Σ_{aa} in $\bar{\Sigma}$.

Call

$$\hat{y}_o = y_o - \mu_b - (\Sigma_{ba}\Sigma_{aa}^{-1})_i(y_i - \mu_i)$$

and denoting $\mathbf{pa}(i)$ with \mathbf{p} ,

$$Z = (\Sigma_{ba}\Sigma_{aa}^{-1})_{-i} \quad C = Z^\top \Sigma_{b|a}^{-1} Z + \Sigma_{pp}^{-1} \quad u^\top = \Sigma_{b|a}^{-1} \hat{y}_o^\top Z \quad \tilde{\mathbf{p}} = \mathbf{p} - \boldsymbol{\mu}_p$$

where $(\Sigma_{ba}\Sigma_{aa}^{-1})_{-i} = \left[\frac{(\Sigma_{ba}\Sigma_{aa}^{-1})_{-i}}{(\Sigma_{ba}\Sigma_{aa}^{-1})_i} \right]$ is a $(p+1) \times 1$ vector with p the number of parent nodes of the intervention variable.

It holds

$$\begin{aligned} & \int_{\mathbb{R}^p} f(y_o | y_i, \mathbf{p}) \tilde{f}(\mathbf{p}) d\mathbf{p} \\ &= \frac{1}{\sqrt{2\pi\Sigma_{b|a}}} \cdot \frac{1}{(2\pi)^{\frac{d}{2}} |\Sigma_{pp}|^{\frac{1}{2}}} \int_{\mathbb{R}^p} \exp \left\{ -\frac{1}{2} (y_o - \boldsymbol{\mu}_{b|a})^\top \Sigma_{b|a}^{-1} (y_o - \boldsymbol{\mu}_{b|a}) - \frac{1}{2} (p - \boldsymbol{\mu}_p)^\top \Sigma_{pp}^{-1} (p - \boldsymbol{\mu}_p) \right\} d\mathbf{p} \\ &\propto \int_{\mathbb{R}^p} \exp \left\{ -\frac{1}{2} \left(\hat{y}_o - (\Sigma_{ba}\Sigma_{aa}^{-1})_{-i} (p - \boldsymbol{\mu}_p) \right)^\top \Sigma_{b|a}^{-1} \left(\hat{y}_o - (\Sigma_{ba}\Sigma_{aa}^{-1})_{-i} (p - \boldsymbol{\mu}_p) \right) \right. \\ &\quad \left. - \frac{1}{2} (p - \boldsymbol{\mu}_p)^\top \Sigma_{pp}^{-1} (p - \boldsymbol{\mu}_p) \right\} d\mathbf{p} \\ &\propto \exp \left\{ -\frac{1}{2} \hat{y}_o^\top \Sigma_{b|a}^{-1} \hat{y}_o \right\} \int_{\mathbb{R}^p} \exp \left\{ -\frac{1}{2} \left[(p - \boldsymbol{\mu}_p)^\top C (p - \boldsymbol{\mu}_p) - 2\Sigma_{b|a}^{-1} \hat{y}_o^\top Z (p - \boldsymbol{\mu}_p) \right] \right\} d\mathbf{p} \\ &\stackrel{(*)}{\propto} \exp \left\{ -\frac{1}{2} \hat{y}_o^\top \Sigma_{b|a}^{-1} \hat{y}_o \right\} \int_{\mathbb{R}^p} \exp \left\{ -\frac{1}{2} \left[(\tilde{\mathbf{p}} - C^{-1}u)^\top C (\tilde{\mathbf{p}} - C^{-1}u) - u^\top C^{-1}u \right] \right\} d\tilde{\mathbf{p}} \\ &\propto \exp \left\{ -\frac{1}{2} \left(\hat{y}_o^\top \Sigma_{b|a}^{-1} \hat{y}_o - u^\top C^{-1}u \right) \right\} \\ &\propto \exp \left\{ -\frac{1}{2} \hat{y}_o^\top \left(\Sigma_{b|a}^{-1} - (\Sigma_{b|a}^{-1}) Z C^{-1} Z^\top (\Sigma_{b|a}^{-1}) \right) \hat{y}_o \right\} \end{aligned} \tag{35}$$

Notice that the domain of the integral is translational invariance, therefore in $(*)$ one could consider $\tilde{\mathbf{p}}$ instead of \mathbf{p} . In addition, since the matrix C is positive definite, the integral

$$\int_{\mathbb{R}^p} \exp \left\{ -\frac{1}{2} \left[(\tilde{\mathbf{p}} - C^{-1}u)^\top C (\tilde{\mathbf{p}} - C^{-1}u) \right] \right\} d\tilde{\mathbf{p}} \propto 1$$

because it is the kernel of a Gaussian distribution with mean $C^{-1}u$ and covariance matrix C^{-1} integrated over its support.

From Eq. (35), it follows that the kernel of the distribution of $\hat{y}_o | \text{do}(Y_i = y_i)$ is

$$\exp \left\{ -\frac{1}{2} \hat{y}_o^\top \left(\Sigma_{b|a}^{-1} - (\Sigma_{b|a}^{-1}) Z C^{-1} Z^\top (\Sigma_{b|a}^{-1}) \right) \hat{y}_o \right\}$$

which corresponds to a $\mathcal{N}(0, \Sigma_{\text{do}})$ with

$$\Sigma_{\text{do}}^{-1} = \Sigma_{b|a}^{-1} - (\Sigma_{b|a}^{-1}) Z C^{-1} Z^\top (\Sigma_{b|a}^{-1}).$$

The expression of Σ_{do} can be extracted from the previous equation using the Sherman-Morrison-Woodbury formula (Higham, 2002, page 258), which states that the inverse of a rank- k modification of a matrix A can be computed by performing a rank- k correction to the inverse A^{-1} . Precisely, the Woodbury formula is

$$A^{-1} - A^{-1}U(B^{-1} + VA^{-1}U)^{-1}VA^{-1} = (A + UBV)^{-1}. \quad (36)$$

where A, U, C and V are conformable matrices: A is $d \times d$, B is $k \times k$, U is $d \times k$ and V is $k \times d$.

Take

$$A = \Sigma_{b|a}, \quad U = Z, \quad B = \Sigma_{pp}, \quad V = Z^\top,$$

it follows

$$\begin{aligned} \Sigma_{\text{do}}^{-1} &= \Sigma_{b|a}^{-1} - (\Sigma_{b|a}^{-1})Z\left(\Sigma_{pp}^{-1} + Z^\top\Sigma_{b|a}^{-1}Z\right)^{-1}Z^\top(\Sigma_{b|a}^{-1}) \\ &= (\Sigma_{b|a} + Z\Sigma_{pp}Z^\top)^{-1} = (\Sigma_{b|a} + (\Sigma_{ba}\Sigma_{aa}^{-1})_{-i}\Sigma_{pp}(\Sigma_{ba}\Sigma_{aa}^{-1})_{-i}^\top)^{-1}. \end{aligned} \quad (37)$$

Recalling $\hat{y}_o = y_o - \mu_b - (\Sigma_{ba}\Sigma_{aa}^{-1})_i(y_i - \mu_i)$, the atomical post-intervention distribution is

$$y_o \mid \text{do}(Y_i = y_i) \sim \mathcal{N}(\mu_{\text{do}}, \Sigma_{\text{do}}) \quad (38)$$

with

$$\begin{aligned} \mu_{\text{do}} &= \mu_o + (\Sigma_{ba}\Sigma_{aa}^{-1})_i(y_i - \mu_i) \\ \Sigma_{\text{do}} &= \Sigma_{bb} - (\Sigma_{ba}\Sigma_{aa}^{-1})\Sigma_{ab} + (\Sigma_{ba}\Sigma_{aa}^{-1})_{-i}\Sigma_{pp}(\Sigma_{ba}\Sigma_{aa}^{-1})_{-i}^\top. \end{aligned} \quad (39)$$

■

A.3 Proof of Proposition 4

Remember that the marginal variance-covariance matrix $\bar{\Sigma}$ of $\bar{\mathbf{Y}} = (\mathbf{pa}(i), y_i, y_o)$ is obtained selecting from Σ the appropriate subset corresponding to the variables $\bar{\mathbf{Y}}$. Since $\bar{\Sigma}$ is still symmetric and positive definite, it also admits a Cholesky factorization. This decomposition of $\bar{\Sigma}$ can be obtained as rank $n - (p + 2)$ downdate of the Cholesky decomposition of Σ , because $n - (p + 2)$ rows and columns from Σ are deleted. However, this procedure is rather complex to perform as the rank of the downdate grows. Therefore, an alternative approach, involving linear SEM properties, is involved in the following proof.

Proof. Without loss of generality, assuming topological ordering, let

$$\bar{\Sigma} = \bar{\mathbf{W}}\bar{\mathbf{V}}^{1/2}(\bar{\mathbf{W}}\bar{\mathbf{V}}^{1/2})^\top$$

be the marginal Cholesky factorization of $\bar{\Sigma}$, the marginal variance-covariance matrix of $\bar{\mathbf{Y}} = (\mathbf{pa}(i), y_i, y_o)$.

Recall that from Wright (1934),

$$(\mathbf{W})_{jh} = (\mathbf{I} - \mathbf{B})_{jh}$$

is the total causal effect of h on j and the diagonal of \mathbf{W} is made by 1's. Integrating out variables not in $\bar{\mathbf{Y}}$ increases the variance, i.e. $\bar{\mathbf{V}}_{jj} \geq \mathbf{V}_{jj}$ for all $j \in \bar{\mathbf{Y}}$, but it does not affect the total effects between remaining variables $\bar{\mathbf{Y}}$. Hence, $\bar{\mathbf{W}}$ is just the sub-matrix $\mathbf{W}_{\bar{\mathbf{Y}}, \bar{\mathbf{Y}}}$ of \mathbf{W} corresponding to variables in $\bar{\mathbf{Y}}$, i.e.

$$\bar{\mathbf{W}}_{hj} = \mathbf{W}_{hj} \quad \text{for all } h, j \in \{\text{pa}(i), i, o\}. \quad (40)$$

From Eq. (12), the elements of the variance in the marginal Cholesky decomposition are given by

$$\bar{\mathbf{V}}_{ii} = 0$$

(in fact, Y_i is enforced to assume the constant value y_i by the do operator) and for $j \in \{\text{pa}(i), o\}$ by

$$\bar{\mathbf{V}}_{jj} = \mathbf{V}_{jj} + \sum_{k < j} \widehat{\mathbf{W}}_{jk}^2 \mathbf{V}_{kk} \quad (41)$$

where Y_k is one of the marginalized nodes and

$$\widehat{\mathbf{W}}_{jk} = \mathbf{W}_{jk} - \sum_{k < h < j} \mathbf{W}_{hk} \mathbf{W}_{jh} \quad (42)$$

with $Y_h \in \bar{\mathbf{Y}}$. Here, $\widehat{\mathbf{W}}_{jk}$ is the weighted (by the path coefficients) number of paths that goes from Y_k to Y_j and do not pass through one of the already considered nodes $Y_h \in \bar{\mathbf{Y}}$ (since the increase in variance carried by that path has already been considered in $\bar{\mathbf{V}}_{hh}$).

Recall $\mathbf{Y}_a = (\mathbf{Y}_{\text{pa}(i)}, Y_i)$ and $\mathbf{Y}_b = Y_o$, writing $\bar{\mathbf{W}}$ and $\bar{\mathbf{V}}$ as block matrix

$$\bar{\mathbf{W}} = \begin{bmatrix} \mathbf{W}_{aa} & \mathbf{0} \\ \mathbf{W}_{ba} & W_{bb} \end{bmatrix} \quad \bar{\mathbf{V}} = \begin{bmatrix} \bar{\mathbf{V}}_{aa} & \mathbf{0} \\ \mathbf{0} & \bar{\mathbf{V}}_{bb} \end{bmatrix},$$

it follows

$$\bar{\Sigma} = \begin{bmatrix} \Sigma_{aa} & \Sigma_{ab} \\ \Sigma_{ba} & \Sigma_{bb} \end{bmatrix} = \begin{bmatrix} \mathbf{W}_{aa} \bar{\mathbf{V}}_{aa} \mathbf{W}_{aa}^\top & \mathbf{W}_{aa} \bar{\mathbf{V}}_{aa} \mathbf{W}_{ba}^\top \\ \mathbf{W}_{ba} \bar{\mathbf{V}}_{aa} \mathbf{W}_{aa}^\top & \mathbf{W}_{ba} \bar{\mathbf{V}}_{aa} \mathbf{W}_{ba}^\top + W_{bb} \bar{\mathbf{V}}_{bb} W_{bb}^\top \end{bmatrix}. \quad (43)$$

Consider the parameters in Eq. (24) of the atomical post-intervention distribution

$$\begin{aligned} \tilde{\mu}_o &= \mu_o + (\Sigma_{ba} \Sigma_{aa}^{-1})_i (y_i - \mu_i) \\ \tilde{\Sigma}_{oo} &= \Sigma_{bb} - (\Sigma_{ba} \Sigma_{aa}^{-1}) \Sigma_{ab} + (\Sigma_{ba} \Sigma_{aa}^{-1})_{-i} \Sigma_{pp} (\Sigma_{ba} \Sigma_{aa}^{-1})_{-i}^\top. \end{aligned} \quad (44)$$

Then

$$(\Sigma_{ba} \Sigma_{aa}^{-1}) = \mathbf{W}_{ba} \bar{\mathbf{V}}_{aa} \mathbf{W}_{aa}^\top \mathbf{W}_{aa}^{-1} \bar{\mathbf{V}}_{aa}^{-1} \mathbf{W}_{aa}^{-1} = \mathbf{W}_{ba} \mathbf{W}_{aa}^{-1}.$$

Since $W_{bb} = 1$, this last quantity corresponds to the last row, except last element, of the inverse $\bar{\mathbf{W}}^{-1}$, which is trivial to compute given the block matrix form. In fact,

$$\bar{\mathbf{W}} = \begin{bmatrix} \mathbf{W}_{aa} & \mathbf{0} \\ \mathbf{W}_{ba} & W_{bb} \end{bmatrix} = \begin{bmatrix} \mathbf{I} & \mathbf{0} \\ \mathbf{0} & W_{bb} \end{bmatrix} \begin{bmatrix} \mathbf{I} & \mathbf{0} \\ W_{bb}^{-1} \mathbf{W}_{ba} \mathbf{W}_{aa}^{-1} & \mathbf{I} \end{bmatrix} \begin{bmatrix} \mathbf{W}_{aa} & \mathbf{0} \\ \mathbf{0} & \mathbf{I} \end{bmatrix},$$

hence

$$\bar{\mathbf{W}}^{-1} = \begin{bmatrix} \mathbf{W}_{aa}^{-1} & \mathbf{0} \\ -W_{bb}^{-1} \mathbf{W}_{ba} \mathbf{W}_{aa}^{-1} & W_{bb}^{-1} \end{bmatrix} = \begin{bmatrix} \mathbf{W}_{aa}^{-1} & \mathbf{0} \\ \mathbf{0} & \mathbf{I} \end{bmatrix} \begin{bmatrix} \mathbf{I} & \mathbf{0} \\ -W_{bb}^{-1} \mathbf{W}_{ba} \mathbf{W}_{aa}^{-1} & \mathbf{I} \end{bmatrix} \begin{bmatrix} \mathbf{I} & \mathbf{0} \\ \mathbf{0} & W_{bb}^{-1} \end{bmatrix}$$

In particular, exploiting again the block form of matrixes, it holds

$$\mathbf{W}_{ba} = [\mathbf{W}_{op} \quad W_{oi}] \quad \mathbf{W}_{bb} = \begin{bmatrix} \mathbf{W}_{pp} & 0 \\ \mathbf{W}_{ip} & W_{ii} \end{bmatrix} \quad \mathbf{W}_{bb}^{-1} = \begin{bmatrix} \mathbf{W}_{pp}^{-1} & 0 \\ -\mathbf{W}_{ip} \mathbf{W}_{pp}^{-1} & w_{ii}^{-1} \end{bmatrix}$$

and therefore

$$(\boldsymbol{\Sigma}_{ba} \boldsymbol{\Sigma}_{aa}^{-1}) = [(\boldsymbol{\Sigma}_{ba} \boldsymbol{\Sigma}_{aa}^{-1})_{-i} \quad (\boldsymbol{\Sigma}_{ba} \boldsymbol{\Sigma}_{aa}^{-1})_i] = \mathbf{W}_{ba} \mathbf{W}_{aa}^{-1} = [\mathbf{W}_{op} \mathbf{W}_{pp}^{-1} - W_{oi} \mathbf{W}_{ip} \mathbf{W}_{pp}^{-1} \quad W_{oi}].$$

This means that

$$\tilde{\mu}_o = \mu_o + (\boldsymbol{\Sigma}_{ba} \boldsymbol{\Sigma}_{aa}^{-1})_i (y_i - \mu_i) = \mu_o + W_{oi} (y_i - \mu_i).$$

Regarding $\tilde{\boldsymbol{\Sigma}}_{oo} = \boldsymbol{\Sigma}_{bb} - (\boldsymbol{\Sigma}_{ba} \boldsymbol{\Sigma}_{aa}^{-1}) \boldsymbol{\Sigma}_{ab} + (\boldsymbol{\Sigma}_{ba} \boldsymbol{\Sigma}_{aa}^{-1})_{-i} \boldsymbol{\Sigma}_{pp} (\boldsymbol{\Sigma}_{ba} \boldsymbol{\Sigma}_{aa}^{-1})_{-i}^\top$, since $W_{bb} = 1$, notice that the terms

$$\begin{aligned} \boldsymbol{\Sigma}_{bb} - (\boldsymbol{\Sigma}_{ba} \boldsymbol{\Sigma}_{aa}^{-1}) \boldsymbol{\Sigma}_{ab} &= \mathbf{W}_{ba} \bar{\mathbf{V}}_{aa} \mathbf{W}_{ba}^\top + \bar{V}_{bb} - \mathbf{W}_{ba} \mathbf{W}_{aa}^{-1} \mathbf{W}_{aa} \bar{\mathbf{V}}_{aa} \mathbf{W}_{ba}^\top = \bar{V}_{bb} \\ (\boldsymbol{\Sigma}_{ba} \boldsymbol{\Sigma}_{aa}^{-1})_{-i} \boldsymbol{\Sigma}_{pp} (\boldsymbol{\Sigma}_{ba} \boldsymbol{\Sigma}_{aa}^{-1})_{-i}^\top &= (W_{op} - W_{oi} \mathbf{W}_{ip}) \bar{\mathbf{V}}_{pp} (W_{op} - W_{oi} \mathbf{W}_{ip})^\top = \tilde{\mathbf{W}}_{op} \bar{\mathbf{V}}_{pp} \tilde{\mathbf{W}}_{op}^\top. \end{aligned}$$

where $\tilde{\mathbf{W}}_{op}$ is a vector $p \times 1$, representing the weighted (by the path coefficients) number of paths that goes from Y_p to Y_o and do not pass through the intervention variable Y_i .

In conclusion

$$\tilde{\boldsymbol{\Sigma}}_{oo} = \bar{V}_{oo} + \tilde{\mathbf{W}}_{op} \bar{\mathbf{V}}_{pp} \tilde{\mathbf{W}}_{op}^\top = V_{oo} + \sum_{l \neq i} (\tilde{W}_{ol})^2 V_{ll} \quad (45)$$

Fixed the intervention variable i , for each outcome variable o in $\{1, \dots, n\} \setminus \{i\}$,

$$\tilde{W}_{ol} = (\mathbf{I} - \tilde{\mathbf{B}})_{ol}^{-1} \quad \text{for all } l \neq i \quad (46)$$

where $\tilde{\mathbf{B}}$ is obtained from matrix \mathbf{B} discarding the effects of the intervention variable, i.e.

$$\tilde{B}_{hj} = \begin{cases} 0 & \text{if } j = i \\ B_{hl} & \text{otherwise.} \end{cases} \quad (47)$$

Moreover, calling $\tilde{\mathbf{V}} = \text{diag}(v_1, \dots, v_{i-1}, 0, v_{i+1}, \dots, v_n)$, the variances of the post-intervention distribution $Y_o \mid \text{do}(Y_i = y_i)$ are given by the diagonal terms of

$$\tilde{\boldsymbol{\Sigma}} = (\mathbf{I} - \tilde{\mathbf{B}})^{-1} \tilde{\mathbf{V}} (\mathbf{I} - \tilde{\mathbf{B}})^{-\top}. \quad (48)$$

■

A.4 Proof of Proposition 5

Proof. Let $\phi(\cdot)$ and $\Phi(\cdot)$ be respectively the p.d.f. and c.d.f. on a standard normal distribution. By Eq. (25), $y_o \mid \text{do}(Y_i = \tilde{y}_i) \sim \mathcal{N}(\tilde{\mu}_o, \tilde{\boldsymbol{\Sigma}}_{oo})$ therefore, its standardization

$$z_o = \frac{y_o - \tilde{\mu}_o}{\sqrt{\tilde{\boldsymbol{\Sigma}}_{oo}}} \sim \mathcal{N}(0, 1).$$

Let $Y_i \sim \mathcal{N}(\mu_i, \sigma_i^2)$ be the marginal distribution of the intervention variable, with $\sigma_i = \sqrt{\Sigma_{ii}}$, and

$$z_i = \frac{\tilde{y}_i - \mu_i}{\sigma_i} \sim \mathcal{N}(0, 1)$$

its standardization.

Call

$$\bar{\alpha}(o, k) = \frac{\alpha(o, k) - \tilde{\mu}_o}{\sqrt{\tilde{\Sigma}_{oo}}} = \frac{\alpha(o, k) - \mu_o}{\sqrt{\tilde{\Sigma}_{oo}}} - \frac{\mathbf{W}_{oi}\sigma_i}{\sqrt{\tilde{\Sigma}_{oo}}} z_i = a_k + bz_i \quad \text{for all } 1 \leq k \leq L_o$$

the standardized outcome thresholds and

$$\bar{\alpha}(i, l) = \frac{\alpha(i, l) - \mu_i}{\sigma_i} \quad \text{for all } 1 \leq l \leq L_i$$

the standardized intervention thresholds. Lastly, let

$$\tilde{a}_k = \frac{a_k}{\sqrt{1+b^2}}, \quad \rho = -\frac{b}{\sqrt{1+b^2}}.$$

Then we have

$$\begin{aligned} & \mathbb{P}\left[Y_o \in [\alpha(o, k-1), \alpha(o, k)] \mid f^{**}(y'_i)\right] - \mathbb{P}\left[Y_o \in [\alpha(o, k-1), \alpha(o, k)] \mid f^*(\tilde{y}_i)\right] \\ &= \int_{\alpha(o, k-1)}^{\alpha(o, k)} \int_{\alpha(i, l'-1)}^{\alpha(i, l')} d\mathcal{N}(y_o, \tilde{\mu}_o, \tilde{\Sigma}_{oo}) f^{**}(y'_i) dy'_i dy_o - \int_{\alpha(o, k-1)}^{\alpha(o, k)} \int_{\alpha(i, l-1)}^{\alpha(i, l)} d\mathcal{N}(y_o, \tilde{\mu}_o, \tilde{\Sigma}_{oo}) f^*(\tilde{y}_i) d\tilde{y}_i dy_o \\ &\stackrel{(*)}{=} \int_{\alpha(i, l'-1)}^{\alpha(i, l')} \int_{\bar{\alpha}(o, k-1)}^{\bar{\alpha}(o, k)} \phi(z_o) dz_o f^{**}(y'_i) dy'_i - \int_{\alpha(i, l-1)}^{\alpha(i, l)} \int_{\bar{\alpha}(o, k-1)}^{\bar{\alpha}(o, k)} \phi(z_o) dz_o f^*(\tilde{y}_i) d\tilde{y}_i \\ &= \int_{\alpha(i, l'-1)}^{\alpha(i, l')} \left[\Phi(\bar{\alpha}(o, k)) - \Phi(\bar{\alpha}(o, k-1)) \right] \frac{1}{\sigma_i} \frac{\phi\left(\frac{y'_i - \mu_i}{\sigma_i}\right)}{\Phi\left(\frac{\alpha(i, l') - \mu_i}{\sigma_i}\right) - \Phi\left(\frac{\alpha(i, l'-1) - \mu_i}{\sigma_i}\right)} dy'_i \\ &\quad - \int_{\alpha(i, l-1)}^{\alpha(i, l)} \left[\Phi(\bar{\alpha}(o, k)) - \Phi(\bar{\alpha}(o, k-1)) \right] \frac{1}{\sigma_i} \frac{\phi\left(\frac{\tilde{y}_i - \mu_i}{\sigma_i}\right)}{\Phi\left(\frac{\alpha(i, l) - \mu_i}{\sigma_i}\right) - \Phi\left(\frac{\alpha(i, l-1) - \mu_i}{\sigma_i}\right)} d\tilde{y}_i \\ &= \int_{\bar{\alpha}(i, l'-1)}^{\bar{\alpha}(i, l')} \left[\Phi(a_k + bz'_i) - \Phi(a_{k-1} + bz'_i) \right] \frac{\phi(z'_i)}{\Phi(\bar{\alpha}(i, l')) - \Phi(\bar{\alpha}(i, l'-1))} dz'_i \\ &\quad - \int_{\bar{\alpha}(i, l-1)}^{\bar{\alpha}(i, l)} \left[\Phi(a_k + bz_i) - \Phi(a_{k-1} + bz_i) \right] \frac{\phi(z_i)}{\Phi(\bar{\alpha}(i, l)) - \Phi(\bar{\alpha}(i, l-1))} dz_i \\ &\stackrel{(**)}{=} \frac{1}{\Phi(\bar{\alpha}(i, l')) - \Phi(\bar{\alpha}(i, l'-1))} \begin{bmatrix} \mathcal{BN}(\bar{\alpha}(i, l'), \tilde{a}_k, \rho) & -\mathcal{BN}(\bar{\alpha}(i, l'-1), \tilde{a}_k, \rho) \\ -\mathcal{BN}(\bar{\alpha}(i, l'), \tilde{a}_{k-1}, \rho) & +\mathcal{BN}(\bar{\alpha}(i, l'-1), \tilde{a}_{k-1}, \rho) \end{bmatrix} \\ &\quad - \frac{1}{\Phi(\bar{\alpha}(i, l)) - \Phi(\bar{\alpha}(i, l-1))} \begin{bmatrix} \mathcal{BN}(\bar{\alpha}(i, l), \tilde{a}_k, \rho) & -\mathcal{BN}(\bar{\alpha}(i, l-1), \tilde{a}_k, \rho) \\ -\mathcal{BN}(\bar{\alpha}(i, l), \tilde{a}_{k-1}, \rho) & +\mathcal{BN}(\bar{\alpha}(i, l-1), \tilde{a}_{k-1}, \rho) \end{bmatrix}, \end{aligned}$$

where we use Fubini-Tonelli theorem to exchange the order of integration in (*) and the following formulas from Owen (1980), where the numbers in parentheses referred to the

formula's number in the paper:

$$\int_h^k \phi(x)\Phi(a+bx)dx = \int_{-\infty}^{\frac{a}{\sqrt{b^2+1}}} \phi(x)\Phi(k\sqrt{b^2+1}+bx)dx - \int_{-\infty}^{\frac{a}{\sqrt{b^2+1}}} \phi(x)\Phi(h\sqrt{b^2+1}+bx)dx \quad (10, 010.4)$$

$$\int_{-\infty}^Y \Phi(a+bx)\phi(x)dx = \mathcal{BN}\left[\frac{a}{\sqrt{1+b^2}}, Y; \rho = \frac{-b}{\sqrt{1+b^2}}\right] \quad (10, 010.1)$$

$$\mathcal{BN}(h, k; \rho) = \begin{cases} \frac{1}{2}\Phi(h) - T\left(h, \frac{k-\rho h}{h\sqrt{1-\rho^2}}\right) + \frac{1}{2}\Phi(k) - T\left(k, \frac{h-\rho k}{k\sqrt{1-\rho^2}}\right) & \text{if } hk > 0, \text{ or if } hk = 0 \text{ and } h \text{ or } k > 0, \text{ or if both } = 0 \\ \frac{1}{2}\Phi(h) - T\left(h, \frac{k-\rho h}{h\sqrt{1-\rho^2}}\right) + \frac{1}{2}\Phi(k) - T\left(k, \frac{h-\rho k}{k\sqrt{1-\rho^2}}\right) - \frac{1}{2} & \text{if } hk < 0, \text{ or if } hk = 0 \text{ and } h \text{ or } k > 0. \end{cases} \quad (3.1)$$

■

A.5 Equivalence of Distribution and Quantile Approach for Truncated Normal Intervention Policies

Although the proof is demonstrated for the toy model in Appendix A.1, it can be easily extended to more general cases involving additional variables with multiple ordinal levels.

$$\begin{aligned} & \mathbb{P}\left[Y_2 \in [\alpha(2, k-1), \alpha(2, k)]\right] |_{f^{**}(y'_1)} - \mathbb{P}\left[Y_2 \in [\alpha(2, k-1), \alpha(2, k)]\right] |_{f^*(\tilde{y}_1)} - \\ &= \int_{\alpha(2, k-1)}^{\alpha(2, k)} \int_{\alpha(1, l'-1)}^{\alpha(1, l')} \frac{1}{\sqrt{2\pi v_2^2}} \exp\left\{\frac{1}{2v_2^2}(y_2 - \mu_2 - b_{12}(y'_1 - \mu_1))^2\right\} f^{**}(y'_1) dy'_1 dy_2 \\ & - \int_{\alpha(2, k-1)}^{\alpha(2, k)} \int_{\alpha(1, l-1)}^{\alpha(1, l)} \frac{1}{\sqrt{2\pi v_2^2}} \exp\left\{\frac{1}{2v_2^2}(y_2 - \mu_2 - b_{12}(\tilde{y}_1 - \mu_1))^2\right\} f^*(\tilde{y}_1) d\tilde{y}_1 dy_2 \end{aligned}$$

(distributional approach)

$$\begin{aligned} & \stackrel{\text{Eq. (29)}}{=} \int_{\alpha(2, k-1)}^{\alpha(2, k)} \int_{\alpha(1, l-1)}^{\alpha(1, l)} \frac{1}{\sqrt{2\pi v_2^2}} \left[\exp\left\{\frac{1}{2v_2^2}(y_2 - \mu_2 - b_{12}(F^{**^{-1}}(F^*(\tilde{y}_1)) - \mu_1))^2\right\} \right. \\ & \left. - \exp\left\{\frac{1}{2v_2^2}(y_2 - \mu_2 - b_{12}(\tilde{y}_1 - \mu_1))^2\right\} \right] f^*(\tilde{y}_1) d\tilde{y}_1 dy_2 \end{aligned}$$

(quantile approach).

(49)

Appendix B. Additional Experimental Results

For the simulations and the analysis we used the R statistical software (R Core Team, 2023, v.4.4.1), where we carried out alternative implementations of the formula in Proposition 5, the first using the numerical integration `integrate` function from the `stats` package, the second exploiting the bivariate normal distribution `pnorm` function from the `mvtnorm` package (Genz and Bretz, 2009, v.1.1-3), and the last using Owen’s T `OwenT` function from the `OwenQ` package (Laurent, 2023, v.1.0.7) for the computations of integrals. Because, as expected, all implementations delivered equivalent results (up to numerical errors) as shown for both the Simulation and the Application to Psychological Data in the Supplementary Material. We present here the results delivered by numerical integration.

B.1 The binary case

In a simplified scenario where we only have two binary variables, without any hidden confounding, we can estimate the average causal effect of the parent node on the child node directly from a contingency table.

Consider two binary variables X_1 and X_2 , whose relationship is described by the following contingency table and X_1 is a direct cause of X_2 .

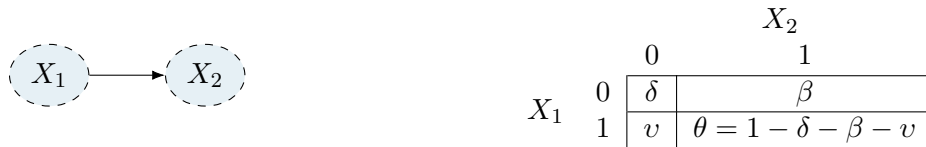


Figure 6: Two binary variable case: DAG (left) and the corresponding contingency table (right).

On the scale of the risk difference, the average causal effects of X_1 on X_2 , are determined as

$$\begin{aligned}
 I_0 &= \mathbb{P}[X_2 = 0 \mid \text{do}(X_1 = 1)] - \mathbb{P}[X_2 = 0 \mid \text{do}(X_1 = 0)] = \frac{v}{v + \theta} - \frac{\delta}{\delta + \beta} \\
 I_1 &= \mathbb{P}[X_2 = 1 \mid \text{do}(X_1 = 1)] - \mathbb{P}[X_2 = 1 \mid \text{do}(X_1 = 0)] = \frac{\theta}{v + \theta} - \frac{\beta}{\delta + \beta}.
 \end{aligned} \tag{50}$$

Alternatively, we may model the relationship between X_1 and X_2 as a latent Gaussian DAG model as defined in Section 2.4. Because 3 independent parameters are sufficient to describe the joint distribution of X_1 and X_2 , a latent Gaussian DAG model can also fully characterise it in terms of the covariance between X_1 and X_2 and the two thresholds that discretize, for each variable, the underlined continuous Gaussian distribution into the two corresponding ordinal levels. Therefore, if our latent model is coherent, we expect it to deliver the same results as those obtained directly from the contingency table. In the following, we verify that assuming a Latent Gaussian DAG model comprising only the intervention and outcome variables (as in the toy model in Appendix A.1) indeed yields the same results. We can express the causal effect on the two levels of X_2 due to an intervention

shifting X_1 from level 0 to level 1 as following, adopting the latent construction described in Eq. (34).

$$\tilde{I}_0 = \mathbb{P}\left[Y_2 \in [-\infty, \alpha_2] \mid \text{do}(Y_1 \in [\alpha_1, +\infty])\right] - \mathbb{P}\left[Y_2 \in [-\infty, \alpha_2] \mid \text{do}(Y_1 \in [-\infty, \alpha_1])\right] \quad (51)$$

$$\tilde{I}_1 = \mathbb{P}\left[Y_2 \in [\alpha_2, \infty] \mid \text{do}(Y_1 \in [\alpha_1, +\infty])\right] - \mathbb{P}\left[Y_2 \in [\alpha_2, \infty] \mid \text{do}(Y_1 \in [-\infty, \alpha_1])\right], \quad (52)$$

where $\mathbf{Y} = (Y_1, Y_2)^\top \sim \mathcal{N}(\mathbf{0}, \boldsymbol{\Sigma})$, b is the given regression coefficient of Y_2 on Y_1 , $\boldsymbol{\alpha} = (\alpha_1, \alpha_2)$ the given thresholds.

Setting $b = 0.5$, $\boldsymbol{\alpha} = (0.2, 0.4)$ and $\mathbf{V} = \mathbf{I}$ one can compute Eq. (51) and Eq. (52) with the previously defined distribution and quantile strategies. We denote these respectively as $(\tilde{I}_{0d}, \tilde{I}_{1d})$ and $(\tilde{I}_{0q}, \tilde{I}_{1q})$.

I_0	\tilde{I}_{0d}	\tilde{I}_{0q}	I_1	\tilde{I}_{1d}	\tilde{I}_{1q}
-0.281642	-0.2816425	-0.2816404	0.281642	0.281642	0.2816419

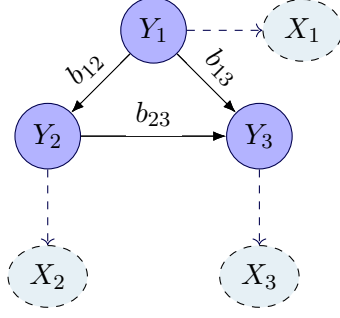
Table 1: Results of causal effect estimation for the binary case.

As shown in Table 1, for two binary variables, the proposed method for computing causal effects determines results in agreement with the causal risk differences. However, this equivalence no longer holds for three or more binary variables. While the latent Gaussian construction can fully characterize the joint distribution of two binary variables, it is well known that no Gaussian distribution can fully represent the unconstrained joint distribution of three or more binary variables. Appendix B.2 illustrates the problem in a case with 3 binary variables. Consequently, the latent Gaussian approach cannot fully capture the distributional properties of ordinal variables, leading to a loss of resolution as dimensionality increases.

Moreover, as proved in Appendix A.5, causal effects $(\tilde{I}_{0d}, \tilde{I}_{1d})$ and $(\tilde{I}_{0q}, \tilde{I}_{1q})$ computed respectively through the distribution and quantile strategies are also equivalent, up to numerical precision in the computation of integrals.

B.2 Three Binary Variables Case

Consider the case of three binary ordinal variables, described by the Latent Gaussian DAG and the following probability tables:



X_1	X_2	X_3	p
0	0	0	τ_0
0	0	1	τ_1
0	1	0	β_0
0	1	1	β_1
1	0	0	γ_0
1	0	1	γ_1
1	1	0	θ_0
1	1	1	θ_1

Figure 7: Three variable case: DAG (left) and the corresponding contingency table (right).

From the previous contingency tables, one can derive:

$$\begin{aligned}
p_{X_1} &= \mathbb{P}(X_1 = 1) = \gamma_0 + \theta_0 + \theta_1 + \gamma_1, \\
p_{X_2,0} &= \mathbb{P}(X_2 = 1 \mid X_1 = 0) = \frac{\beta_0 + \beta_1}{1 - p_{X_1}}, \\
p_{X_2,1} &= \mathbb{P}(X_2 = 1 \mid X_1 = 1) = \frac{\theta_0 + \theta_1}{p_{X_1}}, \\
p_{X_3,0} &= \mathbb{P}(X_3 = 1 \mid X_1 = 0, X_2 = 0) = \frac{\tau_1}{\tau_0 + \tau_1}, \\
p_{X_3,1} &= \mathbb{P}(X_3 = 1 \mid X_1 = 0, X_2 = 1) = \frac{\beta_1}{\beta_0 + \beta_1}, \\
p_{X_3,2} &= \mathbb{P}(X_3 = 1 \mid X_1 = 1, X_2 = 0) = \frac{\gamma_1}{\gamma_0 + \gamma_1}, \\
p_{X_3,3} &= \mathbb{P}(X_3 = 1 \mid X_1 = 1, X_2 = 1) = \frac{\theta_1}{\theta_0 + \theta_1}.
\end{aligned} \tag{53}$$

In analogy with Eq. (50), one can compute the following risk differences

$$\begin{aligned}
I_0 &= \mathbb{P}[X_3 = 0 \mid \text{do}(X_2 = 1)] - \mathbb{P}[X_3 = 0 \mid \text{do}(X_2 = 0)] \\
&= [(1 - p_{X_3,1}) \cdot (1 - p_{X_1}) + (1 - p_{X_3,3}) \cdot p_{X_1}] - [(1 - p_{X_3,0}) \cdot (1 - p_{X_1}) + (1 - p_{X_3,2}) \cdot p_{X_1}]
\end{aligned}$$

$$\begin{aligned}
I_1 &= \mathbb{P}[X_3 = 1 \mid \text{do}(X_2 = 1)] - \mathbb{P}[X_3 = 1 \mid \text{do}(X_2 = 0)] \\
&= [p_{X_3,1} \cdot (1 - p_{X_1}) + p_{X_3,3} \cdot p_{X_1}] - [p_{X_3,0} \cdot (1 - p_{X_1}) + p_{X_3,2} \cdot p_{X_1}]
\end{aligned} \tag{54}$$

and compare with the corresponding differences in latent probabilities obtained from the Gaussian Latent DAG model

$$\tilde{I}_0 = \mathbb{P}\left[Y_3 \in [-\infty, \alpha_3] \mid \text{do}(Y_2 \in [\alpha_2, +\infty])\right] - \mathbb{P}\left[Y_3 \in [-\infty, \alpha_3] \mid \text{do}(Y_2 \in [-\infty, \alpha_2])\right] \tag{55}$$

$$\tilde{I}_1 = \mathbb{P}\left[Y_3 \in [\alpha_3, \infty] \mid \text{do}(Y_2 \in [\alpha_2, +\infty])\right] - \mathbb{P}\left[Y_3 \in [\alpha_3, \infty] \mid \text{do}(Y_2 \in [-\infty, \alpha_2])\right]. \tag{56}$$

I_0	-0.3617032	I_1	0.3617032
\tilde{I}_{0d}	-0.2590655	\tilde{I}_{1d}	0.2590634
\tilde{I}_{0q}	-0.2590577	\tilde{I}_{1q}	0.259063

Table 2: Results of causal effect estimation for the three binary variables case.

Setting $\boldsymbol{\mu} = \mathbf{0}$, $\mathbf{b} = (b_{12}, b_{13}, b_{23}) = (0.5, 0.8, 0.9)$, $\boldsymbol{\alpha} = (1.2, 2.4, 3.3)$ and $\mathbf{v} = (1, 1, 1)$ one gets: As expected, contrary to the previous binary case, it happens that latent probabilities differences in Eq. (55) and Eq. (56) do not match the risk differences in Eq. (54). In fact, it is well known that no Gaussian distribution can fully characterize an unconstrained distribution of three binary variables.

B.3 Simulations

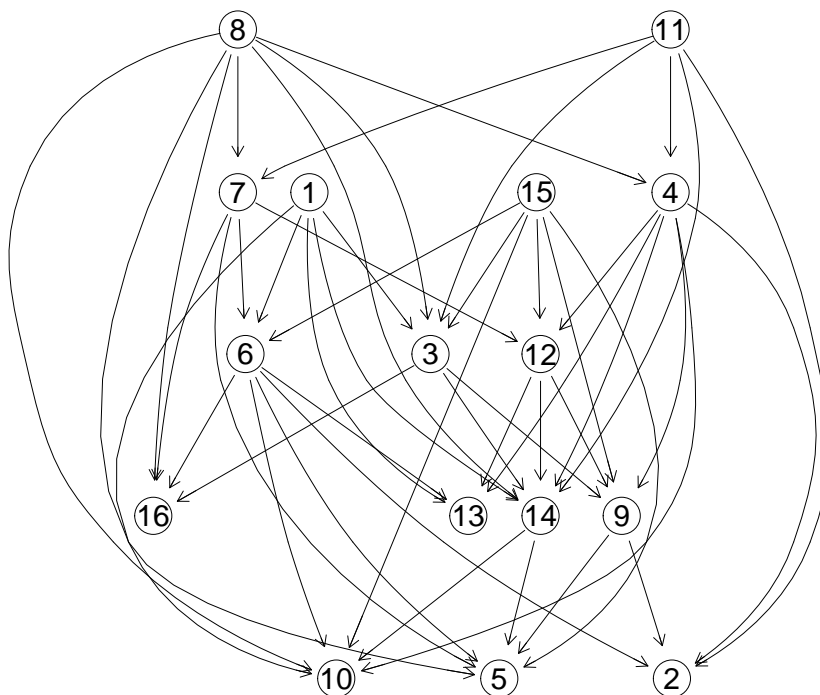


Figure 8: Random E-R DAG with 16 nodes adopted as Latent Gaussian DAG for the simulations.

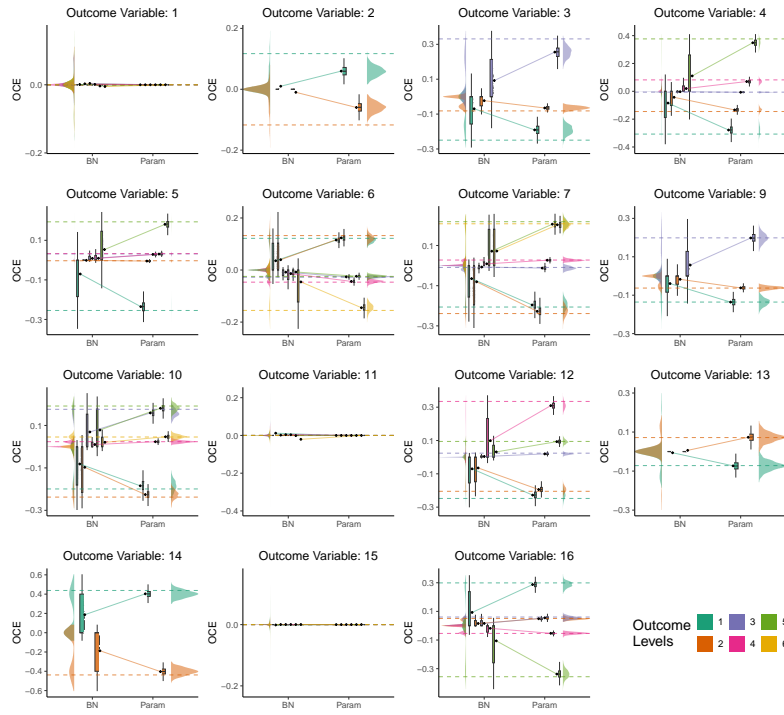


Figure 9: Simulation with Regenerated Data: Ordinal Causal Effects of intervention variable 8.

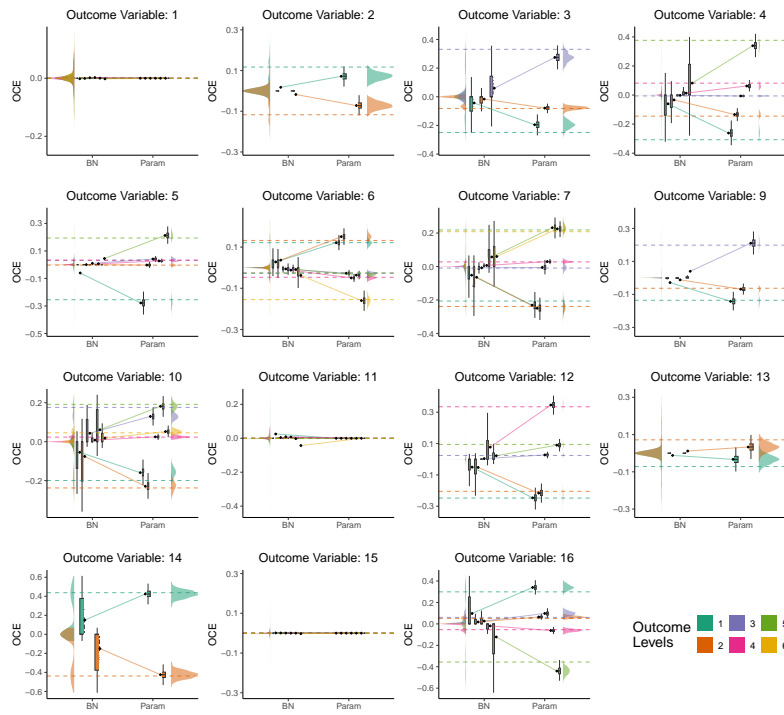


Figure 10: Simulation with Bootstrapped Data: Ordinal Causal Effects of intervention variable 8.

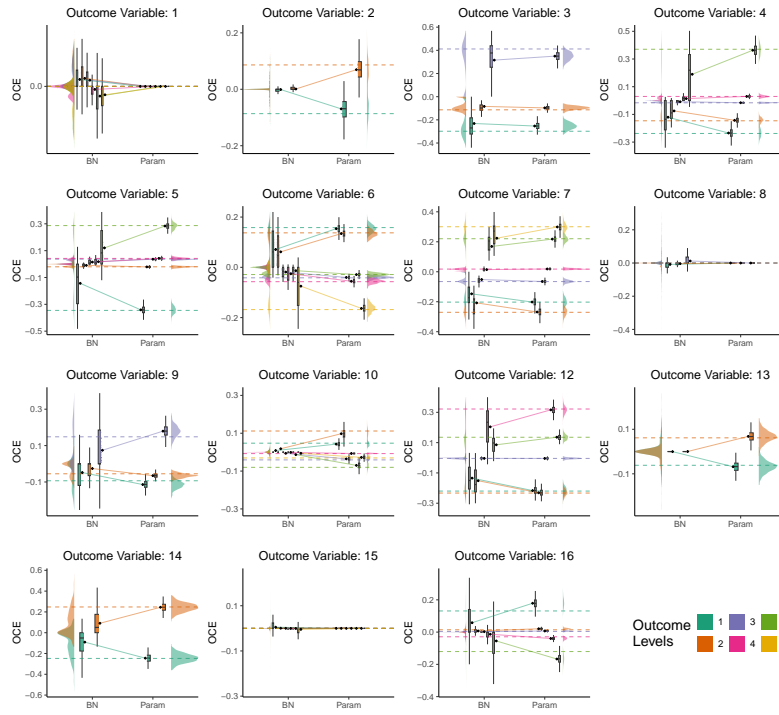


Figure 11: Simulation with Regenerated Data: Ordinal Causal Effects of intervention variable 11.

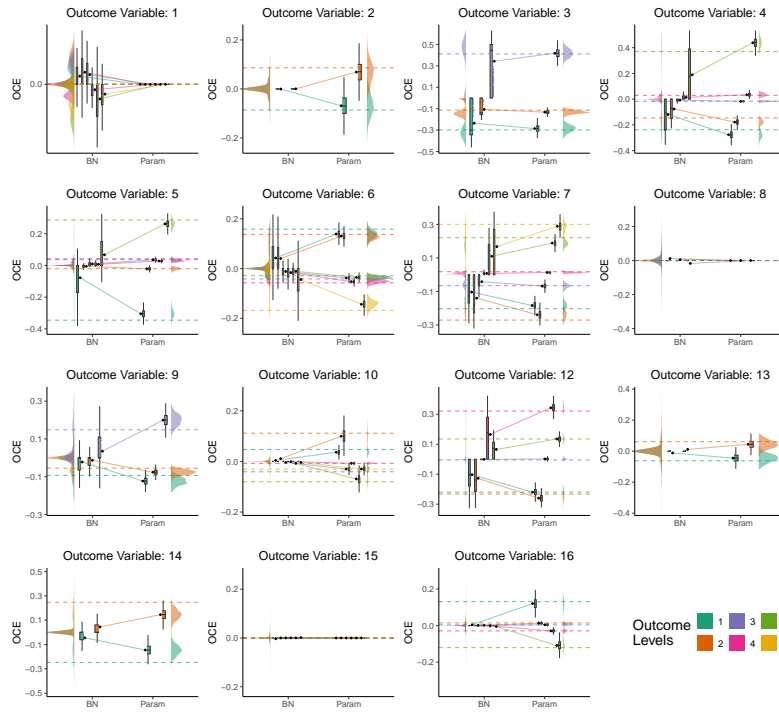


Figure 12: Simulation with Bootstrapped Data: Ordinal Causal Effects of intervention variable 11.

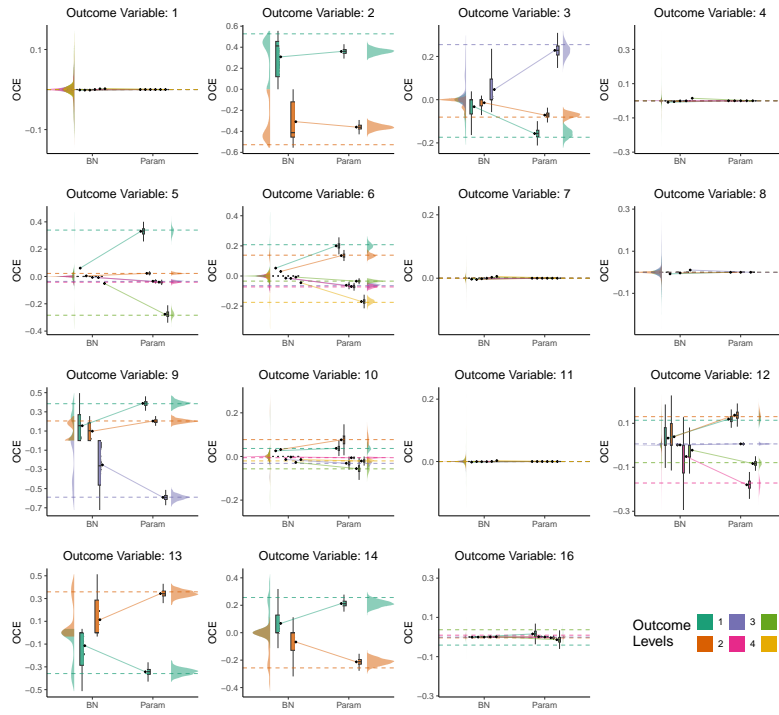


Figure 13: Simulation with Regenerated Data: Ordinal Causal Effects of intervention variable 15.

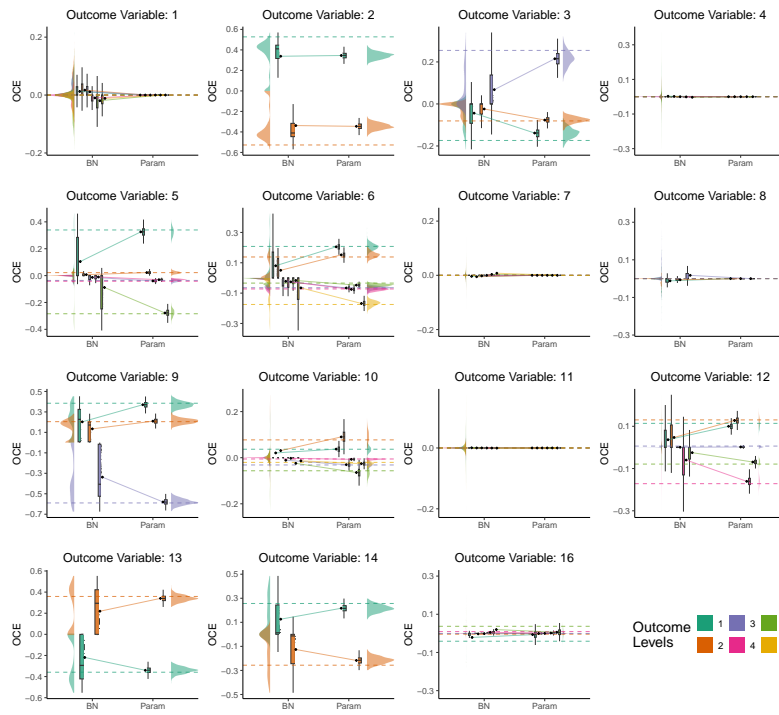


Figure 14: Simulation with Bootstrapped Data: Ordinal Causal Effects of intervention variable 15.

B.4 Analysis of Psychological Data

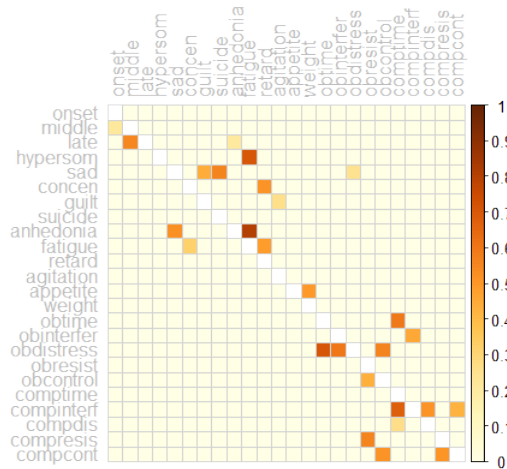


Figure 15: Heatmaps for the CPDAG adjacency matrices of psychological survey data of McNally et al. (2017). The darker the shade in the grid, the more frequently the corresponding directed edge occurs in the 500 Bootstrapped CPDAGs; where an indirect edge counts half for each direction.

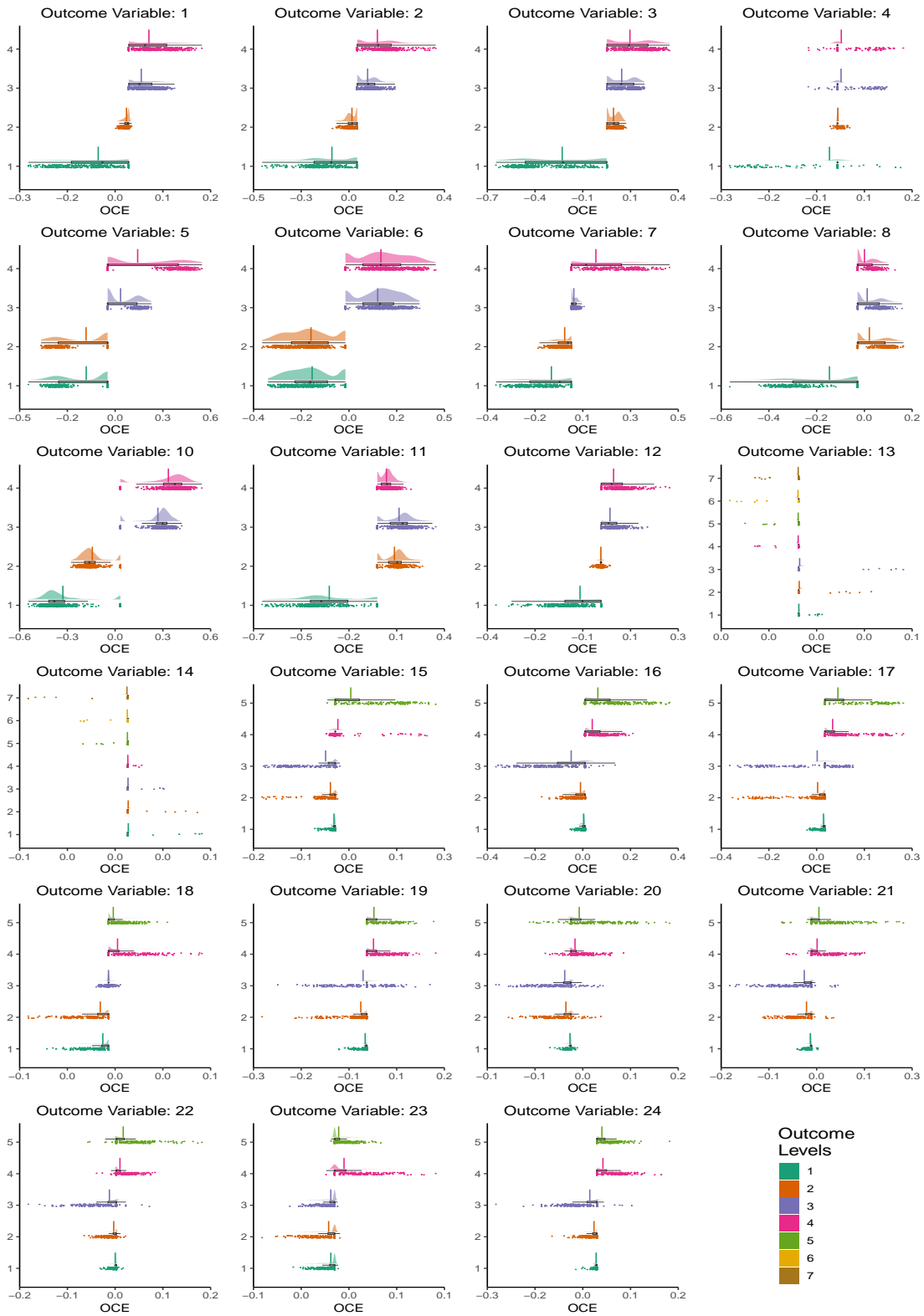


Figure 16: Ordinal Causal Effect of variable 9, resulting from switching it from its lowest to the largest level. The solid lines corresponds to the mean of OCEs for each level of the outcome variable.